

# **Reservoir quality and diagenesis of Triassic sandstones and siltstones from arid fluvial and playa margin environments: a study of one of the UK's earliest producing oilfields**

---

J. C. Scorgie<sup>1</sup>, R. H. Worden<sup>1</sup>, J. E. P. Utley<sup>1</sup>, I. P. Roche<sup>2</sup>

1. Department of Earth Ocean and Ecological Sciences, School of Environmental Sciences, University of Liverpool, 4 Brownlow St, Liverpool, L69 3GP, UK

2. Aurora Energy Resources Limited, Westfield Estate, Milltimber, Aberdeen AB13 0EX

\* contact author [r.worden@liv.ac.uk](mailto:r.worden@liv.ac.uk)

Keywords: East Irish Sea Basin, Sherwood Sandstone Group, Mercia Mudstone Group, reservoir quality, diagenesis, gypsum cement, calcite cement, dolomite cement.

## **Abstract**

The Triassic stratigraphy of the UK contains many major reservoir rock units, present in all major offshore and onshore basins, historically resource rich in oil, gas and water. The Ormskirk Sandstone Formation (Sherwood Sandstone Group) and Tarporley Siltstone Formation (Mercia Mudstone Group) represent the main reservoirs found in one of the UK's earliest producing oilfields at an unusually shallow depth of 30 to 90 m. In this study, environments of deposition present, maximum burial depth, and reservoir quality are evaluated from well Formby-7 using modern analytical techniques. Wireline data and core analysis data were made available by Aurora Energy Resources for the purposes of this study. Formby-7 was continuously cored so that the whole section was logged for sedimentary structures and grain size. Optical analysis of thin sections was conducted, along with SEM-EDS, using thin sections from core plugs. The Ormskirk Sandstone Formation was deposited in a proximal setting by a braided, dryland river with aeolian influence; the Tarporley Siltstone Formation was deposited in a more distal setting on the margins of a playa environment. The study found that the reservoir quality is excellent in the deeper Ormskirk sediments, but relatively poor in the overlying Tarporley sediments. Good reservoir quality present in the Ormskirk Sandstone Formation is linked to early depositional textures, grain size (medium sand) and general lack of pore-filling cements. In the Tarporley, reservoir quality is poor due to the grain size (very fine sand) and the variable presence of pore-filling gypsum associated with playa deposits. Minor feldspar diagenesis (both dissolution and precipitation) occurred in both the Sherwood and Mercia sediments. The small degree of mechanical compaction and lack of any signs of mesodiagenesis suggest that the clastic sediments in the Formby-7 well have not been buried deeper than about 1,000 m. The findings reported here can be used to

help the understanding of UK Triassic sedimentology and reservoir quality for oil and gas, geothermal energy, CCS (carbon capture storage) and water supply.

# 1 Introduction

Active oil seeps have long been reported in the area north of Liverpool, NW England, UK, near the town of Formby. The first known record of an oil seep was described in 1637 when local people reportedly used oil-soaked wood or peat as a source of fire-lighting material and for medicinal uses on livestock (Craig et al., 2018). The seeps were later rediscovered by Binney and Talbot (1869), and were thought to be sourced from the breakdown of algae within the overlying peat deposits (Roche, 2012). During the 1930s, the search for oil in the UK was accelerated due to the realisation that Europe was heading towards conflict. Renewed geological surveying by Cope (1939) prompted exploratory drilling at Formby by D'Arcy Exploration Company (the forerunner to BP) (Roche, 2012). The second well, Formby-G2, resulted in the discovery of the shallow Formby Oilfield (Figs. 1 and 2) with mobile oil within the Quaternary Shirdley Hill Sandstone and underlying Lower to Middle Triassic sediments (Craig et al., 2018). The diminutive Formby oilfield produced a total 71,557 barrels of oil from 1939 to the eventual abandonment of field in 1965 (Minchin et al., 2005). The exploration in the East Irish Sea Basin led to the discovery in 1974 of the giant South Morecambe gas field. Later exploration led to the discovery and development of several large conventional oil and gas fields (Lennox, Hamilton, Douglas) that are 10 to 30 kilometres offshore from the Formby oilfield (Bunce, 2018; Yaliz and Chapman, 2003; Yaliz and Taylor, 2003; Yaliz, 1997). These offshore fields are sourced from the same Carboniferous petroleum system as the onshore Formby oilfield (Pharaoh et al., 2016). Several conventional onshore wells have been drilled in the Formby area since abandonment of the Formby oilfield, most recently by Aurora Energy Resources (Roche, 2012; Roche and Openshaw, 2011) who drilled the Formby-MFA-1 which is the focus of this study, in 2012. Well Formby-MFA-1 is also referred to as Formby-7 (Leppard, 2012) and L110/15-81 (UK OGA block and well name).

Permian and Triassic sediments are major reservoir and aquifer rocks that are present in many sedimentary onshore and offshore basins around the UK, with the Wytch Farm oilfield in the Wessex Basin (Bowman et al., 1993; McKie et al., 1998), Lennox oil and gas field in the East Irish Sea Basin, to name a few (Yaliz and Chapman, 2003). There have been many studies of Permo-Triassic reservoir and aquifer rocks, with the Lower Triassic Sherwood Sandstone Group undergoing extensive study since it is important for fresh water supply (Holloway et al., 1989), geothermal energy sources (Allen and Holloway, 1984; Downing et al., 1984), oil and gas production (Bowman et al., 1993; Burley, 1984; Hogg et al., 1996; Meadows and Beach, 1993; Schmid et al., 2004) and most recently as a possible host for carbon capture and storage (Armitage et al., 2016, 2013; Newell et al., 2008).

The Lower Triassic Sherwood Sandstone Group sediments present in the Formby oilfield provide an analogue for possible offshore carbon capture and sequestration in stratigraphically identical rocks in the East Irish Sea oil and gas fields (Holloway, 2009). They also represent an analogue for the exploration of geothermal resources in the Sherwood Sandstone aquifer in the nearby Cheshire Basin (Hirst et al., 2015).

The Middle to Upper Triassic Mercia Mudstone Group has been studied extensively as a top-seal (Armitage et al., 2013, 2011; Seedhouse and Racey, 1997). However, little has been published on the reservoir potential of Mercia Mudstone Group sedimentary rocks since they have typically been reported to be a “waste” zone, for example in the Lennox and Hamilton oil and gas fields (Yaliz and Taylor, 2003). The Tarpoley Siltstone Formation, within the Mercia Mudstone Group in the Formby Oilfield, may represent an analogue for these hitherto ignored zones, especially in areas where oil exploration is revisiting previously overlooked or ignored strata.

Direct comparisons of specific formations found in the Formby Oilfield to similar rocks in other areas can be difficult due to (i) the diachroneity of sediments in the micro- and macro-fossil deficient Triassic, and (ii) different local formation names for the same stratigraphy (Fig. 3). Ambrose et al. (2014) and Howard et al. (2008) recognised this problem and sought to correct complexity of Triassic nomenclature. Although some discrepancies remain between offshore and onshore units, a common nomenclature was established by Haig et al. (1997) as shown in Figure 3.

This paper aims to address the following questions:

1. What were the environments of deposition of the Ormskirk Sandstone Formation and Tarporley Siltstone Formation in the Formby oilfield?
2. What are the dominant controls on the reservoir quality of the Ormskirk Sandstone Formation and Tarporley Siltstone Formation in the Formby oilfield?
3. What can be inferred about the burial and geological history of reservoirs in the Formby oilfield?
4. What are the implications of modern reservoir studies of the Formby Oilfield for both future oil and gas exploration and the transition to a low carbon economy (geothermal, carbon sequestration and water supply)?

## **2 Geological Background**

The Formby Oilfield is located on the eastern fringes of the structurally complex East Irish Sea Basin (Figs. 1 and 2). Formby sits within the West Lancashire Basin which is a sub-basin of the East Irish Sea Basin. The East Irish Sea Basin (EISB) is one of the most significant sedimentary basins found in the United Kingdom, due to the extensive ( $\leq 5,000$  m) thicknesses of sand-rich

Permian-Triassic sedimentary rocks that overlie significant thicknesses of fine-grained, organic-rich Carboniferous source rock sediments (Fig. 4) (Rowley and White, 1998).

The West Lancashire Basin developed during two main phases of rifting in a NNW-SSE trending fault system (Fig. 1b), that extended from the Wessex Basin in South West England to the Hebrides off in north west Scotland (Swann and Munns, 2003). The first phase of rifting occurred during the Early Carboniferous (Dinantian, 359 to 326 Ma); major growth faults in the region developed in response to a regional extension in the East Irish Sea Basin (Rowley and White, 1998). Rifting ceased towards the Late Dinantian, indicated by sedimentary fill evidence (Rowley and White, 1998). This was followed by a period of thermal subsidence during the Middle to Upper Carboniferous (Namurian and Westphalian, 326 to 304 Ma) represented by deposition of marine shales (Jackson et al., 1987; Jackson and Mulholland, 1993; Rowley and White, 1998). A second phase of east-west rifting started during the Permian with regional stretching (NE-SW and ENE-WSW) evident in the EISB (Jackson and Mulholland, 1993). Normal faulting and syn-tectonic sedimentation occurred during this phase as evidenced by significant variations in thickness of Permo-Triassic deposits adjacent to faults (Rowley and White, 1998). For example, Permian and Triassic deposits are significantly thicker to the west of the Formby Point Fault (EISB/West Lancashire Basin margin) compared to the eastern deposits in the West Lancashire Basin (Fig. 4) (Yaloz and Chapman, 2003). By the Lower Triassic, the isolated sub-basins of the East Irish Sea Basin (Cheshire Basin, Solway Firth Basin and West Lancashire Basin) had coalesced into one single depocentre (Rowley and White, 1998). Fault-controlled sedimentation locally continued into the Jurassic in parts of the East Irish Sea Basin, as evidenced by the presence of Jurassic sediments in the hanging walls of some faults, however, is likely to have been insignificant compared with Jurassic rifting seen elsewhere in the UK such as the North Sea (Jackson and Mulholland,

1993). There are no Jurassic, or younger, sediments in the Formby area of the West Lancashire Basin; Middle to Upper Triassic Mercia Mudstone Group deposits are the youngest rocks to sub-crop beneath recent Quaternary deposits, as illustrated in Figure 5 (Rowley and White, 1998; Yaloz and Chapman, 2003). The Triassic sedimentary rocks at the surface in west Lancashire, approximately 30 km north of Formby, have reportedly undergone intermediate burial to approximately 1000 m, before being uplifted to their current stratigraphic position (De Pater and Baisch, 2011).

The Lower Triassic sediments in the East Irish Sea Basin are collectively known as the Sherwood Sandstone Group; these sediments have been locally subdivided into various formations. At the Formby oil field, the sandstone is known as either the Ormskirk Sandstone Formation or the Helsby Sandstone Formation, depending on whether the reference is to the offshore (oil field) or onshore (outcrop) terminology (Fig. 3). Here we will use the stratigraphic term Ormskirk Sandstone Formation to refer to the deeper and coarser sandstone unit within the Formby-7 well, to avoid confusion and to clarify the relevance of the sandstones in the oil field to the large number of onshore Sherwood outcrops in the UK from as far south as Sidmouth in Devon, England to as far north as Burghead in Moray, Scotland.

The Middle and Upper Triassic sediments in the East Irish Sea Basin are collectively known as the Mercia Mudstone Group; these sediments have also been locally subdivided into various formations. At the Formby oil field, the Mercia Mudstone is known as the Tarporley Siltstone Formation by reference to onshore (outcrop) terminology from the Cheshire Basin (Earp and Taylor, 1986). Here we will use the stratigraphic term Tarporley Siltstone Formation to refer to the shallower and finer-grained unit within the Formby-7 well, instead of using the term



Mercia Mudstone, because the Tarporley Siltstone is silt- and sand-grade, rather than mud-grade sediment.

### 3 Methods and materials

#### 3.1 Log Data and Analysis

The Formby-MFA-1 well (Formby-7; Fig. 5) had a standard sets of downhole log data collected: caliper (CAL), gamma (GR), density (RHOB), neutron (NPHI) and deep resistivity (RD).

For the overall interpretation of lithology and fluid saturation, porosity was initially derived from the density log using equation 1.

$$\text{Porosity } (\phi_{\text{RHOB}})\% = 100 \cdot \frac{\rho_{\text{ma}} - \rho_{\text{b}}}{\rho_{\text{ma}} - \rho_{\text{fl}}}$$

(Equation 1)

Where  $\rho_{\text{ma}}$  is the assumed matrix (rock) density,  $\rho_{\text{b}}$  is the measured bulk rock density (RHOB) and  $\rho_{\text{fl}}$  is the assumed fluid density for the invaded zone of the near well-bore region (approximately 1 g/cm<sup>3</sup>). Values of  $\rho_{\text{b}}$  (matrix density) were slightly varied to optimise the fit of the reservoir section core analysis porosity to the derived density log porosity; 2.64 g/cm<sup>3</sup> was used as the grain density of the Ormskirk Sandstone Formation and 2.73 g/cm<sup>3</sup> was used as the grain density of the Tarporley Siltstone Formation, reflecting the elevated quantity of mica and gypsum in the siltstone compared to the sandstone. Following Beaumont et al. (2019) to deal with shale-rich reservoirs, we compared the density-derived porosity to the neutron porosity. For logged-intervals where the density-derived porosity was greater than the reported neutron porosity (NPHI), then we used the density-derived porosity. For logged-

intervals where the density-derived porosity was less than the reported neutron porosity we used equation 2 (Beaumont et al., 2019).

$$\text{Porosity } (\phi_{\text{shale-corrected}} \%) = 100 \cdot \left[ \frac{\phi_{\text{RHOB}}^2 + \text{NPHI}^2}{2} \right]^{0.5}$$

(Equation 2)

The solid part of the rock can split into proportions of shale and sand using normalised gamma log data and the Vshale calculation (equation 3).

$$V_{\text{shale}} = \frac{GR_b - GR_{\text{min}}}{GR_{\text{max}} - GR_{\text{min}}}$$

(Equation 3)

Where  $GR_{\text{max}}$  is the maximum gamma value for the reservoir-top-seal section of interest,  $GR_b$  is the measured gamma value for the depth of interest and  $GR_{\text{min}}$  is the minimum gamma value for the reservoir-top-seal section of interest.

The fluids in the pore space have been divided into water and petroleum using the deep resistivity log and equation 4, a shale-corrected version of the Archie equation, known as the Indonesia equation (Shedid and Saad, 2017).

$$S_{W_{\text{Indonesia}}} = \left\{ \frac{\sqrt{\frac{1}{R_d}}}{\left( \frac{V_{sh}^{(1-0.5V_{sh})}}{\sqrt{R_{sh}}} \right) + \sqrt{\frac{\phi^m}{a \cdot R_w}}} \right\}^{2/n}$$

(Equation 4)

Where  $S_{w_{Indonesia}}$  is the shale-corrected fractional water saturation,  $a$ ,  $m$  and  $n$  are the Archie constants (default values: 1, 2 and 2 but modified here to fit  $S_w$  to as close to 1.00 as possible in the water leg),  $\phi$  is the porosity determined using either the density log (equation 1) or the shale-corrected porosity (equation 2), and  $R_d$  is the deep resistivity of the formation.  $R_{sh}$  is the resistivity of shale in the reservoirs, which was reported to be 5 ohm.m at the time of drilling. Formation water (groundwater) salinity was assumed to be 30,000 ppm salinity in the evaporite-rich Tarporley Siltstone and 5,100 ppm salinity in the carbonate-rich Ormskirk Sandstone Formation in the Sherwood Sandstones. The lower salinity in the deeper but more permeable Ormskirk Sandstone Formation probably reflects active meteoric flow. Water table contours get progressively deeper moving from south to north of the north Liverpool/west Lancashire region (Mohamed and Worden, 2006) proving there is an active flow system. These salinity values led to formation water resistivity values of 0.2515 ohm.m at 15.6 °C for the Tarporley Siltstone and 1.3 ohm.m at 15.6 °C for the Ormskirk Sandstone Formation.

In terms of mineral chemistry,  $V_{shale}$  reveals the total quantity of radioactive minerals in rock; this is often treated as being the same as the total quantity of clay minerals since these are typically dominated by radioactive potassium-bearing illite (and mixed layer illite-smectite). Strictly speaking,  $V_{shale}$  therefore represents the quantity of illite and smectite (assuming the  $GR_{min}$  value accounts for the quantity of radioactive potassium-bearing K-feldspar) as opposed to the quantity of all clays (noting that chlorite and kaolinite are non-radioactive).

The neutron log represents the total quantity of hydrogen in the rock, and thus includes pore fluids in the invaded near-well bore zone and hydroxyl-bearing clay minerals (and any other H-bearing mineral such as gypsum or zeolite). The absolute  $N_{shale}$  value ( $N_{shale_{abs}}$ ) can be derived using equations 5 and 6, by subtracting the percentage porosity, determined from the

density log (equation 1), from the neutron, the result revealing the relative quantity of clay minerals:

$$\text{Nshale}_{\text{abs}} = \text{NPHI} - \phi_{\text{RHOB}}$$

(Equation 5)

Where NPHI is the percentage neutron log signal and  $\phi_{\text{RHOB}}$  is the density log-derived porosity. The  $\text{Nshale}_{\text{abs}}$  values vary about zero. To normalise the data and make them comparable to Vshale values, we used:

$$\text{Nshale} = \frac{\text{Nshale}_{\text{abs-b}} - \text{Nshale}_{\text{abs-min}}}{\text{Nshale}_{\text{abs-max}} - \text{Nshale}_{\text{abs-min}}}$$

(Equation 6)

Where  $\text{Nshale}_{\text{abs-max}}$  is the maximum  $\text{Nshale}_{\text{abs-max}}$  value for the reservoir-top-seal section of interest,  $\text{Nshale}_{\text{abs-b}}$  is the measured  $\text{Nshale}_{\text{abs}}$  for the depth of interest and  $\text{Nshale}_{\text{abs-min}}$  is the minimum  $\text{Nshale}_{\text{abs}}$  value for the reservoir-top-seal section of interest.

The difference between Vshale (relative quantity of radioactive clay minerals) and Nshale (relative quantity of all clay minerals) should reveal the relative proportions of radioactive illite (plus any smectite) versus the non-radioactive clay minerals, such as kaolinite plus chlorite, or other H-bearing minerals.

### **3.2 Core Analysis**

The whole well was cored. Core analysis was performed by ALS Petrophysics (Guildford) and the data were made available by Aurora Energy Resources. Sixty core plugs for routine core analysis were drilled taken parallel to bedding and a further nine vertical core plugs (perpendicular to bedding) were chosen for additional Dean and Stark analysis. Porosity was

calculated using a standard porosimeter with inert, gas phase nitrogen. Permeability was measured using the flow of inert, gas phase nitrogen gas at a confining pressure of 400 psi. Core plug grain density was calculated by measuring the mass, diameter and length of each plug. Core analysis porosity data are accurate to within 0.5 %.

### ***3.3 Core Description***

Core and sample material (museum core, half slab core, cuttings and core plugs) were obtained with permission from Aurora Energy Resources. The Mesozoic cored interval from Formby MFA-1 (L110/15-81) was logged between the intervals of 24.8 m to 94.2 m over five days at the ALS core store in Guildford for lithology, facies variations, grain size and sedimentary structures. Grain size was measured at regular intervals by comparing core material to standard grain size charts.

### ***3.4 Petrography***

Twenty standard polished thin sections were prepared from core plugs cleaned to remove live and residual oil. No special precautions were used to dry and clean the samples as precedent from Triassic sandstones have shown they do not contain collapsible clay mineral fabrics. Optical photomicrographs were captured using an Olympus BX51 light optical microscope, fitted with an Olympus SC50 digital camera. Modal data were collected from a Leica DM 2700P microscope fitted with a Petrog<sup>®</sup> setting stage. Detrital grains, cements and porosity were quantified using point counting based on 200 counts, with both porosity and solid grains included in the same channel. Grain size data was collected with 100 counts on the longest axis. A carbon coat was applied to the polished sections prior to SEM analysis.

### **3.5 SEM-EDS**

Quantitative evaluation of mineral proportions and mineral-based petrographic imaging were undertaken using SEM-EDS, which consists of an automated, spatially-resolved petrography system, based within a scanning electron microscope, using energy-dispersive X-ray spectroscopy detectors and an extensive mineral database (Armitage et al., 2010; Pirrie et al., 2004). SEM-EDS analyses give quantitative mineral proportions, grain and pore space morphology and distribution, to a minimum resolution of  $\sim 1 \mu\text{m}$  (the smallest beam-sample interaction volume width). SEM-EDS cannot identify or quantify microporosity and it struggles to quantify any mineral grain that is smaller than about 1 or 2  $\mu\text{m}$ . The SEM-EDS instrument used in this study was an FEI WellSite QEMSCAN at the University of Liverpool, using a tungsten-filament, operating at 15 kV, equipped with two Bruker EDS detectors (Wooldridge et al., 2018). SEM-EDS data are accurate to within fractions of a percent.

### **3.6 X-ray Diffraction (XRD)**

Sub-samples of core plug samples 1 (33 m) and 8 (60.91 m) that were interpreted to contain abundant calcium sulphate were dry crushed to a powder  $< 10 \mu\text{m}$  using a stainless-steel centrifuge ball mill. Samples were back-loaded into cavity holders as random powders. Samples were then scanned in a PANalytical X'Pert Pro MPD X-ray diffractometer. Copper X-rays were used, with a Ni filter to select for Cu  $k\text{-}\alpha$  radiation. Scans covered the  $2\theta$  range of 4 to  $70^\circ 2\theta$ . Operation of XRD was undertaken using "HighScore Plus<sup>®</sup>" analysis software; quantification used the Relative Intensity Ratio (RIR) method with reference patterns from: International Centre for Diffraction Data, Powder Diffraction File-2 Release 2008.

## 4 Results

### 4.1 Wireline log data

The caliper, gamma, density, neutron and deep resistivity logs are shown in Figure 6. The borehole size, revealed by the caliper log, was somewhat bigger than the size of the drill bit (Fig. 6A) suggesting that the sedimentary rock was relatively unconsolidated or susceptible to washing out during drilling. Some thin zones have washed out intensively suggesting that there may be local layers that are especially weak, or especially liable to be affected by water in the drilling mud (e.g., especially rich in water soluble minerals).

The gamma ray log (Fig. 6B) shows a major difference between the Ormskirk Sandstone Formation and the Tarporley Siltstone Formation with the former having a low gamma response and the latter having a higher and highly heterogeneous gamma profile. The Ormskirk Sandstone Formation looks as if it is lithologically broadly homogeneous in terms of the gamma log response. The Tarporley Siltstone Formation appears to be variable on a metre-scale. The variations could be depositional (i.e., beds) or they result from secondary diagenetic processes.

The density and neutron log data are plotted on a cross-over diagram (Fig. 6C) with opposite scales on the X-axes. These diagrams are typically used for reservoir evaluation to reveal the cross-over areas (Rider and Kennedy, 2011). Where the density log is to the left of the neutron log, then the interval is assumed to be relatively porous (net pay). Where the density log is to the right of the neutron log, then the interval is assumed to have low porosity and is classed as non-net pay (non-reservoir). The density-neutron cross-over diagram (Fig. 6C) illustrates the major difference between the Ormskirk Sandstone Formation, deeper than 69 m, and the Tarporley Siltstone Formation. The Ormskirk Sandstone Formation seems to represent

uniformly good reservoir but there seem to be only thin intervals of good quality reservoir in the relatively heterogeneous Tarporley Siltstone Formation.

The resistivity log displays increasing values up-section in the low gamma, good quality reservoir in the deeper Ormskirk Sandstone Formation suggesting that the upper part may be oil-bearing and the lower part may be water-bearing. The overlying Tarporley has some high resistivity values in the lower gamma, lower density intervals (e.g. at 40 m) suggesting that the cleaner parts of the Tarporley may be oil-bearing.

The logs have been interpreted to produce a better understanding of the reservoir intervals in the Formby-7 well.  $V_{shale}$ , representing the total of all radioactive clay minerals such as illite and smectite, has been determined using equation 3, revealing the uniformly sandy character of the Ormskirk interval and the metre-scale heterogeneity of the Tarporley Siltstone Formation (Fig. 7B).

$N_{shale}$  has been determined using equations 4 and 5, where  $N_{shale}$  represents the total of all clay minerals and all other H-bearing minerals,  $N_{shale}$  and  $V_{shale}$  have been directly compared in Figure 7B. In intervals where  $N_{shale}$  far exceeds  $V_{shale}$ , e.g. at various depths in the Tarporley Siltstone, there is either an excess of non-radioactive clay minerals (e.g. kaolinite or chlorite) or an excess of another H-bearing minerals such as gypsum; these options will be examined when we present the mineralogy data.

We have determined simple reservoir properties and the lithology of the reservoir section by first deriving porosity using equation 1 and then deriving the proportions of oil and water in the pore space using equation 2. The solid portion of the rock was then split into sandstone and shale using  $V_{shale}$ , derived using equation 3 and plotted in Figure 7A and 7B. The resulting plot neatly displays the presence of oil versus water and sand versus shale (Fig. 7C). The



Ormskirk Sandstone Formation, in the deeper part of the section is oil-filled at its top but there is an oil-water transition zone deeper than about 90 m. Porosity in the Ormskirk Sandstone Formation tends to be lowest where the  $V_{shale}$  shows a small increase (e.g., at 85 m) suggesting that depositional sand-mud proportions exert a significant control on reservoir quality.

The Tarporley Siltstone Formation has lower maximum porosity values than the Sherwood but there are some 2 to 3 m, fining upward intervals (e.g. 52 to 49 m) that are oil-filled. The highest porosity in the Tarporley occurs in intervals that have the lowest  $V_{shale}$  contents, suggesting that reservoir quality is primarily a function of depositional sand versus mud concentrations. However, the Tarporley interval between 69 and 62 m generally gets less shale rich up-section, but the porosity does not increase. This suggests that there must be a secondary control on reservoir quality. It is notable that  $N_{shale}$  increases from 69 to 62 m but  $V_{shale}$  decreases suggesting that either non-radioactive clay minerals or other H-bearing minerals such as gypsum control reservoir quality in the upper part of this interval.

The relationships between  $N_{shale}$ , reservoir quality and stratigraphy are illustrated in Figure 8 in which we have plotted density-log derived porosity (equation 1) as a function of depth, varied symbol size by  $V_{shale}$  (equation 3) and symbol colour by  $N_{shale}$  (equation 5). There is a marked difference between the good reservoir quality sandstones in the Ormskirk Sandstone Formation and the Tarporley Siltstone Formation with the former having a lower  $N_{shale}$  (red hues) than the latter (yellow to green hues). Even for low  $V_{shale}$ -high porosity Tarporley samples there is a relatively high  $N_{shale}$  reinforcing the interpretation that either non-radioactive clay minerals or other H-bearing minerals such as gypsum are present in the Tarporley Siltstone Formation.

## **4.2 Core analysis**

Core analysis porosity from both the Lower Triassic Ormskirk Sandstone Formation and overlying Mid Triassic Tarporley Siltstone Formation are shown in Appendix 1, and Figures 7, 9 and 10. In the Ormskirk Sandstone Formation porosity ranges between 17 and 32 %, and permeability ranges between 500 and 9,000 mD.

The porosity in the Tarporley Siltstone Formation varies between 8 and 20 %, and the permeability varies between just greater than the detection limit of the permeameter (0.01) to 110 mD.

Core analysis porosity values have been plotted on the diagrams illustrating reservoir properties and the lithology of the reservoir (Fig. 7C). The log-derived porosity values match well the lab-measured core porosity values.

## **4.3 Core description**

Sedimentary core logs from Formby MFA-1 can be seen in Figures 9 (Ormskirk Sandstone Formation) and 10 (Tarporley Siltstone Formation). Rubble at the very top of the core (24.18 to 24.70 m) is boulder clay from Quaternary sediment, which has not been included in this study.

### **4.3.1 Ormskirk Sandstone Formation**

The Sherwood Sandstone can be identified within the cored section between depths of 69.10 to 94.23 m (Fig. 9). This unit is locally known as the Ormskirk Sandstone Formation, which is the lateral equivalent of the Helsby Sandstone Formation that outcrops 40 km to the south-southwest (near Frodsham in Cheshire) and 30km to the south-southeast (near Thurstaston in the Wirral) (Fig. 3).

The unit is comprised of generally homogeneous sandstones with a distinct lack of mud- or silt-grade sediment (Figs. 11A and B). The core is heavily oil stained, with visible porosity present throughout most of the core. The Ormskirk Sandstone Formation varies from fine- to coarse-grained, normal and reverse grain size grading in beds, and bedding structures varying from absent, to finely laminated, cross-bedded and cross-laminated, and current rippled. The colour of the core can be used for discrimination due to the heavy oil staining. The Ormskirk Sandstone Formation was here split into four facies present in the cored section on the basis of grain size and sedimentary structure (Fig. 9): (i) aeolian dune facies, which is fine to coarse grained, is identified by high angle and cross stratification and grain flow laminae (Fig. 11B), defined by reverse grading (coarsening up ) on the cm-scale, (ii) fluvial channel fill facies, which is medium to coarse grained with common cross lamination and current ripples and minor carbonaceous (coal like) material, (iii) sand-flat facies, characterised by medium to coarse grain size, and either fine mm-scale (5 to 10 mm) laminations or an apparent lack of bedding (Fig. 11A) and (iv) sand-sheet facies, which are fine to medium grained that locally display mm-scale (5 mm) laminations.

#### **4.3.2 Tarporley Siltstone Formation**

The Tarporley Siltstone Formation is present in the cored section between depths of 24.70 to 69.10m (Fig. 10). This stratigraphic interval is heterogenous and is comprised of pinstripe silt- and mud-stones, with thin beds of slightly coarser grained siltstone and fine sandstone (Figs. 11C and D). Facies identified within the Tarporley siltstone unit include playa lake facies and sheet flood facies.

Playa lake facies sediments are typically silt and mud. Syneresis cracks are present within the muddier intervals. The siltier intervals exhibit fine wave ripple laminations. Veins or nodules of gypsum common (Fig. 11C).

Sheet flood facies sediments are typically silt- to fine-sand grade. Sheetflood facies are often finally laminated, with some areas showing evidence of current ripple lamination. Minor hydrocarbon shows are present within some sheet flood beds.

#### **4.4 Petrography**

Petrographic analysis of the Ormskirk Sandstone Formation revealed that samples are moderately- to well-sorted, with modal grain size varying from lower fine sand to upper medium sand grade (Fig. 12, Appendix 3). QFL analysis from point count data showed that the Ormskirk Sandstones are predominantly sub-lithic or quartz arenites, with only one sample identified as a sub-feldspathic arenite (Fig. 13). The Ormskirk Sandstones are predominately comprised of detrital quartz (Figs. 12A, 12C, 12E), K-feldspar and plagioclase (Fig. 12G), with minor lithic fragments (Fig. 12G). There are dolomite-rich lithic grains that were probably reworked phreatic dolomite cements (Figs. 12A, 12B) (Spötl and Wright, 1992; Worden, 1998; Worden et al., 1999; Worden and Matray, 1998). Clay minerals are rare and, where present, appear to be detrital in origin (Fig. 12C), as opposed to diagenetic; this interpretation is made as clay minerals were present prior to early gypsum cement emplacement, suggesting they were deposited during deposition. There are small quantities of dolomite cement present up to 11 % (Fig. 12 C). Minor euhedral pyrite is observed in trace quantities up to 0.5 %. Residual oil staining is common throughout in varying quantities up to 7 %, appearing as a green non-birefringent layer (Figs. 12 C and E). Some quartz grain underwent quartz cementation during an earlier event, with the overgrowths displaying unusually rounded terminations and a non-

euohedral outline proving that sedimentary transport occurred following initial burial, heating, quartz growth, uplift and erosion. These second cycle quartz overgrowths are present in trace amounts up to 3 % (Fig. 12C). We cannot be certain, but it is likely that these second cycle quartz cements were derived from Namurian sandstones, now exposed as hard, quartz cemented rocks in the Pennine mountain chain, 50 to 100 kms to the east of the Formby site of deposition. Feldspar cements (intragrowths and overgrowths) are also found to be present in trace amounts up to 0.5 %. Primary porosity, varying from 12.5 to 20.5 %, is the dominant type of porosity with minor quantities of secondary isolated and secondary connected porosity up to 0.5 %.

The Tarporley Siltstone Formation is well- to very well-sorted, with modal grain size varying from lower very fine to upper very fine sand (Fig. 14, Appendix 3). Six of the seven samples classify as feldspathic arenite, and one sample was identified as a sub-lithic arenite. Detrital grains within the Tarporley Siltstone Formation are predominantly comprised of detrital quartz (Figs. 14A, 14C, 14E, 14G) varying from 28 to 49.5 %. Detrital plagioclase and K-feldspar are also present with quantities between 12 and 30.5 % present, with some samples containing a small quantity of rigid volcanic rock fragments up to 8% (Fig. 14E). Blocky cements present are predominantly gypsum (Fig. 14A) up to 34 %. Calcite cements (Fig. 14F) are also present up to 10 %, with second cycle quartz cements identified (Fig. 14E) up to 2.5 %. Feldspar cements (intragrowths and overgrowths) are also present in varying quantities up to 3.5 %. Euhedral pyrite can also be found in quantities ranging from trace to 1.5 % throughout (Fig.13G). Detrital clays are present in varying amounts up to 32.5 % (Figs. 14G, 14H). Traces of residual staining can be found in samples with visible pore space up to 2 % (Fig. 14C). The quantity of primary porosity in the Tarporley Siltstone Formation is between 0 and 7.5 % (Fig.

14E), with isolated secondary porosity also present from the dissolution of unstable framework grains up to 2.5 % (Fig. 14F).

## **4.5 SEM-EDS Mineralogy**

SEM-EDS mineral quantification was undertaken on 20 Ormskirk Sandstone Formation samples and eight Tarporley Siltstone Formation samples. Modal SEM-EDS data are given in Appendix 4, normalised data are plotted on Figures 9 and 10. SEM-EDS images of the Ormskirk Sandstone Formation are shown in Figures 12B, 12D, 12F and 12H, and of the Tarporley Siltstone Formation are shown in Figures 14B, 14D, 14F and 14H.

### **4.5.1 Ormskirk Sandstone Formation mineralogy**

In the Ormskirk Sandstone Formation, quartz can be assumed to be entirely detrital since the quantity of inherited quartz overgrowths is less than 3 % (Fig. 12E). SEM-EDS analyses (Appendix 4, Figs. 9 and 12) show that quartz is the dominant detrital mineral (75 to 90 %), quartz cements were recorded during petrographic analysis, but were deemed to be second cycle quartz (i.e. detrital) (Fig. 12E). K-feldspar is the second most abundant mineral ranging 7 to 10 % (Figs. 12B, 12D, 12F, 12H), with much lower quantities of plagioclase feldspar ranging from 0.6 to 3 % (Figs. 12D, 12F, 12H). However, both quantities cannot differentiate between detrital and authigenic feldspar that were recorded in section 4.4. Small quantities of muscovite (0.2 to 0.6 %) and trace quantities of biotite (< 0.05 %) are present. Heavy minerals rutile and apatite are present in trace quantities (values of 0.09 to 0.29 % respectively). Dolomite (0.7 to 2.4 %) and Fe-dolomite (0.5 to 1.6 %) are present throughout the Sherwood sandstone (Figs. 12B, 12D, 12F, 12H) although petrographic images (Figs. 12A, 12B, 12F and 12H) reveal that at least some of the dolomite may be present as lithic grains (reworked

dolomite from interfluvial (in the Lower Triassic) as opposed to mineral cement. The most volumetrically important clay mineral is illite (1 to 3.5 %) with minor traces (< 0.1 %) of kaolinite, smectite and chlorite.

#### **4.5.2 Tarporley Siltstone Formation mineralogy**

In the Tarporley Siltstone Formation, SEM-EDS analyses (Figs. 10 and 14, Appendix 3) show that quartz is the dominant detrital mineral (41 to 72 %) (Figs. 14B, 14D, 14F, 14H). K-feldspar represents the second most abundant detrital mineral (10 to 13 %), with smaller quantities of detrital plagioclase feldspar (4 to 8 %), although SEM-EDS cannot differentiate between lithic present and authigenic feldspar cements seen during petrographic analysis. Ductile detrital minerals include muscovite (1 to 6 %) and biotite (0.5 to 3.5 %) (Fig. 14F). Rutile (Figs. 14D, 14F) and apatite are the dominant heavy minerals (values ranging between 0.43 and 0.82 %, respectively). Dolomite and Fe-dolomite are less abundant than in the Sherwood Sandstone (0.1 to 3.6 %) but calcite is more abundant (0.02 to 2.9 %). Calcium sulphate (noting that SEM-EDS cannot differentiate between gypsum and anhydrite) is present in large quantities (up to 25 %) but it is not ubiquitous throughout the Tarporley Siltstone (Figs. 14B, 14D, 14F) and up to 2.5 % pyrite (Fig. 14D). Clay minerals are also variable, with chlorite (up to 0.5 %), kaolinite (up to 0.5 %) and illite (1 to 14 %) (Fig. 14H), present throughout the Tarporley Siltstone.

#### **4.6 XRD mineralogy**

XRD analyses of samples 1 (33 m) and 8 (60.91 m), from the Tarporley Siltstone Formation, confirmed that calcium sulphate, quantified and imaged using SEM-EDS (Figs. 10, 14B, 14D and 14F, Appendix 4), is gypsum ( $\text{CaSO}_4 \cdot 2\text{H}_2\text{O}$ ) and not anhydrite.

## 5 Discussion

The stratigraphy in the Formby area was previously described by Kent (1948) and Leppard (2012). The stratigraphy present in the Formby oilfield consists of Lower Triassic Ormskirk Sandstone Formation deposits (Figs. 3 and 9) and Middle Triassic Tarporley Siltstone Formation (Figs. 3 and 10) deposits.

Ormskirk Sandstone Formation sediments are identified in wireline logs from low gamma with a high neutron-density crossover (Fig. 6C). V-shale and N-shale (Figs 7A and 7B) are low in the Ormskirk Sandstone Formation sediments, indicating that clay minerals are largely absent, as supported by the SEM-EDS data (Figs. 9 and 12).

The Tarporley Siltstone Formation is identified in wireline by high gamma (Fig. 6B), subsequently leading to a high V-shale fraction (Fig. 7B, 7C). This shows that clay minerals are relatively abundant, as supported by the SEM-EDS data (Figs. 10 and 14).

### ***5.1 Environments of deposition***

#### **5.1.1 Ormskirk Sandstone Formation reservoir**

The core description, petrography and log characteristics all suggest that the Ormskirk Sandstone Formation was deposited in a dryland river/fluviol to aeolian environment (Fig. 15A). Trough cross-bedding, current ripples, grain size (Fig. 9C) and the presence of dolomite intraclasts (Figs. 12A-B) suggest that the majority of the Ormskirk succession represents fluvial deposition in a semi-arid setting (Holloway et al., 1989; Schmid et al., 2006).

Localised grain-fall laminae (alternating cm-scale laminae) (Fig. 11B, 12D) represent deposition by aeolian dunes (Jones and Ambrose, 1994). Trough cross bedding (likely fluvial in



origin) possibly represents reworking of aeolian dune deposits, also recognised elsewhere in equivalent Triassic sediments (Meadows and Beach, 1993).

There have been similar interpretations for the depositional environments for Sherwood Sandstone (Ormskirk Sandstone Formation) equivalent to sediments at Formby in the Carlisle Basin to the north, Cheshire Basin to the south, and the Isle of Man Basin to the north-west (Jones and Ambrose, 1994).

### **5.1.2 Tarporley Siltstone Formation reservoir**

The core description, petrography and log characteristics all suggest that the Tarporley Siltstone Formation was deposited in a marginal playa-sandflat environment (Fig. 15B). The presence of siltstones and fine-grained-sandstones interbedded on the metre-scale, minor wave ripples in the siltstones, current ripples in the fine-grained sandstones (Fig. 10C), localised mm-scale (pin-stripe) bedding of mudstone and gypsum, desiccation cracks filled with gypsum (Figs. 10C, 11C, 14A-D), all suggest deposition close to the margins of a playa system. The fine-grained sandstone was probably deposited in a sheet-flood and the siltstone was deposited in an ephemeral lake.

The lithology is representative of cyclic depositional events of mudstone (playa lake facies) and sandstone (sheet flood facies) deposition (Fig. 15B). Playa lake facies are characterised by bedding with a mud to silt grade grain size. Veins of gypsum (Fig. 11C) are interpreted to be the result of desiccation formed during periods of drought (Plummer and Gostin, 1981). The gypsum present within the thin mudstone beds are likely to have resulted from evaporation of saline playa-lake waters soon after deposition (Schmid et al., 2003).

The sandstone beds present in the Tarporley Siltstone Formation are often small in scale, being often less than a metre in thickness. It is likely that due to the minimal thicknesses of

these beds that they would have been deposited by sudden events, likely due to flooding of the playa lake (Tunbridge, 1984). This is graphically displayed in the accumulation of sediment Figure 15B. The cyclic nature of the sandstone beds observed in the Tarporley Siltstones are likely to be linked to periodic climate variations. The interbedding and Tarporley Siltstone Formation sandstone and siltstone at Formby (Fig. 11) presented a challenge for recovery of petroleum. Given the small areal size of the field, the reservoir required an unusually large number of wells (Roche and Openshaw, 2011) to extract the resource probably because of the stratigraphic compartmentalisation of the upper Tarporley Siltstone Formation reservoir.

The clear distinction between the Ormskirk Sandstone Formation and Tarporley Siltstone Formation, evident in the wireline logs (Figs. 6-8) and sedimentary logs (Figs 9-10), suggests an abrupt change from fluvial-aeolian to playa lake dominated environments. This may imply that there is an unconformity between the Ormskirk Sandstone Formation and Tarporley Siltstone Formation.

## ***5.2 Controls on reservoir quality of the Ormskirk Sandstone Formation and Tarporley Siltstone Formation***

Understanding the controls on porosity and permeability (reservoir quality) is typically an essential part of any initial study into petroleum reservoirs. However, the same approach and principles to understanding porosity and permeability are applicable to other fast-developing sectors. For example, carbon capture sequestration (CCS) are being planned in rocks of Lower to Middle Triassic age in the UK (Armitage et al., 2016, 2013; Kirk, 2005). Geothermal energy exploitation is being planned in the Cheshire Basin from Lower to Middle Triassic sandstones (Hirst et al., 2015). Understanding the flow properties of aquifers is also important for water

resource management with the Sherwood sandstone commonly used as a type-example of a fluvial sandstone aquifer (Medici et al., 2019).

In Formby MFA-1, reservoir quality is different between the Lower Triassic Ormskirk Sandstone Formation and Middle Triassic Tarpoley Siltstone Formation, as evident in wireline logs (Fig. 6-8), core data (Figs. 9-11) and thin section evidence (Figs. 12, 14). In the Ormskirk Sandstone Formation, porosity is visually high in core and thin section (Figs. 11A, 11B and 12). In wireline logs this is revealed by high density-log porosity (Figs. 6C, 8 and 9F) and a substantial neutron-density crossover (Fig. 6C). In the Tarpoley Siltstone Formation, density-log porosity is comparatively low, whilst neutron-density crossover reveals that much of the section is non-pay (Fig. 6C).

### **5.2.1 Sequence of reservoir quality-affecting processes**

Reservoir quality is typically a consequence of a combination of depositional (grain, size, sorting, matrix clay) and diagenetic (compaction, dissolution and cementation) processes (Worden et al., 2018; Worden and Burley, 2003). The sequence of events that lead to porosity-modification can be interpreted using petrographic data (Figs. 16-17).

The Ormskirk Sandstone Formation paragenetic sequence is very simple (Fig. 16). The degree of compaction is not strong, as evidenced by the open pores in all petrographic images (Fig. 12). Early diagenetic cements are represented by early ferroan dolomite growth (Fig. 12B-C). Subsequent localised dissolution of unstable framework grains (mainly volcanic lithic fragments and feldspar grains) had a chance to alter the pore network (Figs 12F-G). Minor pyrite grew, probably after the grain dissolution event. Oil emplacement seems to have been the last process since oil coats all grains and all cements. A diagram comparing compactional and cementational porosity-loss (Fig. 18) confirms that cementation has not been a major

control on reservoir quality for the Ormskirk Sandstone Formation. Figure 18 also shows that compaction has occurred because the visible macro-porosity is less than 20 %, which is lower than the initial, depositional, porosity of probably a little greater than 40 % (Beard and Weyl, 1973). The lack of strong compaction and the small volume of cement suggests that these rocks have not been deeply buried (probably < 1,000 m). The lack of burial of this area has been reported elsewhere (De Pater and Baisch, 2011).

The Tarporley Siltstone Formation paragenetic sequence is slightly more complex than the one for the Sherwood Sandstone (Fig. 17). The quantity of gypsum cement and matrix clay minerals (Fig. 14) means that compactional porosity-loss in the sand intervals is not easy to assess. However, deformed micas are present in the Tarporley sandstone intervals showing that some compaction has probably occurred (Fig. 14E). The earliest diagenetic event was calcite growth, and possibly dolomite growth (Fig. 14D-F). These carbonate cements were followed by gypsum cement (Figs. 14A-D). There was some subsequent dissolution of unstable framework grains (feldspar and minor volcanic grains) (Figs. 14C and F). There was a small degree of K-feldspar cementation as overgrowths on detrital grains. The last mineral cement to grow was pyrite (Figs. 14C, D, G). Oil emplacement seems to have been the last process since oil coats all grains and all cements. The diagram comparing compactional and cementational porosity-loss (Fig. 18) confirms that cementation has been a major control on reservoir quality for much of the Tarporley Siltstone Formation. The most abundant cement is gypsum showing that clastic deposition in playa margin settings can lead to poor reservoir quality due to early diagenetic precipitation of gypsum.

### 5.2.2 Ormskirk Sandstone Formation reservoir quality

The core analysis porosity of the Ormskirk Sandstone Formation varies from 17 % to 29 % (Figs. 9F, 19, 20). Based on comparison of the core analysis data to the SEM-EDS data (Fig. 9), and point count data (Appendix 1), there is no apparent way, in terms of mineralogy, cement content, detrital grain type or grain size, to account for the 12 % difference in porosity between the best and the worst Ormskirk Sandstone Formation samples in terms of reservoir quality. There is also no simple relationship between the higher porosity Ormskirk samples and wireline-derived Vshale or Nshale (Figs. 19A and B). Comparison of the core porosity and the degree of compactional porosity-loss, derived using the approach defined by Houseknecht (1987) (Fig. 21), it is apparent that the 12 % difference in porosity is probably due to different degrees of compaction. It is not clear why there are different degrees of compaction but possible explanations may include localised zones of enhanced deformation (Griffiths et al., 2018) or telogenetic dissolution (Worden et al., 2018) and removal of a transient evaporative cement (Strong, 1993) that limited that extent of compaction during burial.

The core analysis permeability of the Ormskirk Sandstone Formation varies from ~ 200 mD to ~ 9 D (Figs. 9F, 19, 20). There is no simple relationship with porosity. Comparison of the core data to the wireline data reveals that, for a given porosity, permeability increases with decreasing Vshale (and Nshale) (Fig. 19), suggesting that a decreasing quantity of clay minerals leads to elevated permeability (Appendix 4). The core analysis data are poorly differentiated by depositional environment (facies) in the Ormskirk Sandstone Formation (Fig. 20A). There is a great degree of overlap in the porosity and permeability values for the four identified facies; the reasons for this will be explored later. When the core data are graded by petrographic grain size sorting, it is also apparent that for a give porosity, permeability increases with increasing grain size and better sorting (Fig. 20B). The relationship between

sorting and permeability is also emphasised in Figure 22. Finally, permeability is highest in Ormskirk Sandstone Formation samples that have the lowest sum total of authigenic minerals (defined by point-counting) and matrix (Fig. 22).

To address the question of lateral continuity of sandstone reservoir quality, we have compared Formby to the Lennox field. The Ormskirk Sandstone Formation reservoir quality in the Formby oil field (Figs. 19, 20B) is distinctly better than the same sandstone in the nearby Lennox oilfield (Haig et al., 1997). The Formby-Ormskirk Sandstone Formation maximum and median porosity values are about 5% higher and the media permeability is about one order of magnitude higher than the same sandstone in Lennox. Thus, while it is certain that the reservoir sandstones extend well over 10 kms to the west, reservoir quality decreases, probably due to the greater depth of Lennox at the present day and the greater maximum palaeo-depth.

### **5.2.3 Tarporley Siltstone Formation reservoir quality**

The core analysis porosity of the Tarporley Siltstone Formation varies from 8 % to 20 % (Figs. 10F, 19, 20). Based on comparison of the core analysis data to the SEM-EDS data (Fig. 10), and point count data (Appendix 1), there is a good inverse correlation between the sum total of pore-filling minerals (carbonates, gypsum, pyrite, illite, smectite and chlorite) and core analysis porosity (Appendix 4). There is a fairly good inverse correlation between gypsum and core analysis porosity as gypsum is the dominant pore-filling cement (Figs. 14B, D and F). These patterns are reinforced by the point count data (Appendix 1).

The core analysis data for the two different depositional environments (facies) in the Tarporley Siltstone Formation overlap to a great degree (Fig. 20A) showing that factors other than depositional processes must control reservoir quality. There is no simple relationship

between grain size and core analysis porosity: the finest Tarporley Siltstone Formation sample has the smallest grain size (Fig. 20B).

There is no simple relationship between the lower porosity Tarporley samples and wireline-derived  $V_{\text{shale}}$  given that some of the lowest porosity samples have very low  $V_{\text{shale}}$  (Fig. 19A). In contrast,  $N_{\text{shale}}$  values tend to increase with decreasing core analysis porosity reinforcing the dominant control of gypsum on Tarporley Siltstone Formation reservoir quality (Fig. 19B).

Based on comparison of the Tarporley Siltstone Formation core porosity and the degree of compactional porosity-loss, derived using the approach defined by Houseknecht (1987) (Fig. 21), it is apparent that the 12 % difference in porosity is not due to different degrees of compaction. This is in direct contrast to the Ormskirk Sandstone Formation. Instead, the 12% difference in porosity between the best and the worst of the Tarporley Siltstone Formation seems to be due to the presence of pore-filling gypsum or matrix. Matrix was present immediately after deposition and it is likely that gypsum precipitated from evaporating playa lake waters and was also present soon after deposition showing that both matrix and gypsum will have inhibited compaction.

The core analysis permeability of the Tarporley Siltstone Formation varies from  $< 0.01$  to 110 mD (Figs. 10F, 19, 20). There seems to be a relatively simple relationship with porosity. There is a good inverse correlation between the sum total of pore-filling cements plus matrix and permeability (Fig. 22; Appendix 1).

**5.2.4 The lowest porosity sections in the Tarporley Siltstone Formation, with values as low as about 10 %, probably represent the top-seal of the Formby oil field. The seeps that abound in the geographical area**

**prove that the seal is not perfect. Shale-rich sections with 10% porosity are to be expected given the shallow burial of the section. Comparison of Tarporley and Ormskirk reservoir quality**

The porosity and permeability data for the Ormskirk Sandstone Formation and the Tarporley Siltstone Formation seem to present a good and continuous correlation (Figs. 19 and 20B). However, any attempt to construct one correlation curve for the entire porosity-permeability database would be wrong as the Ormskirk Sandstone Formation and the Tarporley Siltstone Formation are fundamentally different types of sediment with different controls on reservoir quality. In terms of first order controls on reservoir quality, the Ormskirk Sandstone Formation is medium grained, with negligible matrix and only minor eodiagenetic dolomite cement; in contrast the Tarporley Siltstone Formation is silt grade with either abundant matrix or abundant eodiagenetic gypsum cement (Table 2). It has been demonstrated that both sand-grade and silt-to-mud-grade sediment have porosity and permeability evolution trends (Cade et al., 1994; Neufelder et al., 2012) that are primarily controlled by grain size and it is fundamentally incorrect to correlate materials that have different grain sizes. This also relates to the concept of flow-zone indicator whereby it is inappropriate to try to correlate rocks with pore size distributions (Tiab and Donaldson, 2015).

The Ormskirk Sandstone Formation is clearly a better reservoir quality unit than the Tarporley Siltstone Formation (Table 2, Figs. 9, 10, 19, 20B). These differences are reflected in wireline log data (Figs. 6, 7, 8), core analysis data (Figs. 9F and 10F), mineralogy data (Figs 9G, 10G) and petrographic images (Figs. 12, 14). The Ormskirk Sandstone Formation is coarser grained (Figs. 20B, 21, 22), and has less matrix, carbonate cement and gypsum cement than the Tarporley Siltstone Formation (Figs. 19, 20B, 22). It is significant that the range of porosity in the Ormskirk Sandstone Formation has here been interpreted to be the result of different degrees



of compaction (Figs. 18, 21). The different degrees of Ormskirk Sandstone Formation compactional porosity-loss may be the result of dissolution of earlier gypsum or carbonate cement due to aquifer flow (Strong, 1993). The overlying Tarporley Siltstone Formation still has abundant gypsum cement, presumably due to the less massive character of the sandstones in the Tarporley Siltstone Formation, which inhibited flow of water and subsequent dissolution.

### ***5.3 Interpreted burial and geological history of reservoirs in the Formby oilfield?***

The Ormskirk Sandstone Formation has undergone a minor degree of compaction; thin section images (Fig. 12) show that the majority of grain-contacts are point contacts, with some samples containing floating grains. There are no signs of mesodiagenesis for either the Ormskirk Sandstone Formation or the Tarporley Siltstone Formation proving that these rocks have not been to temperatures in the mesogenetic realm (i.e they have definitely not been in excess of 70 to 80 C (i.e., they have not been buried to 3,000 m).

Burial history modelling of the East Irish Sea Basin has been conducted by Cowan et al. (1999) and De Pater and Baisch (2011). Cowan et al. (1999) concluded that offshore of the Formby oil field in the East Irish Sea Basin, Sherwood Sandstone sediments have been buried to a maximum depth of approximately 3,000 m (Cowan et al., 1999). De Pater and Baisch (2011) modelled burial of equivalent sediments at Preese Hall, near Weeton in Lancashire, approximately 30 km north of Formby, and concluded that the Sherwood Sandstone sediments have been buried to a depth of approximately 1,000 to 1,500 m before uplift to the surface at the present-day.

The large-scale cross section in Figure 4 shows that there is at least 1,000 m of Mercia Mudstone Group sediment in the East Irish Sea, ~ 10 km to the west of Formby. Assuming the Mercia had roughly uniform thickness across the region, then this suggests that the sediments at Formby have been buried at least 1,000 m deeper than they are at the present day since the Mercia Mudstone Group sediments at Formby are only 40 m thick.

In summary, the reservoirs at Formby have been buried to greater than 1,000 m but probably less than 2,000 m.

#### ***5.4 Significance for future oil exploration and alternative energy sources (geothermal and carbon sequestration).***

The Ormskirk Sandstones at Formby can be used as an analogue for relatively clean sands that have undergone apparently minor eodiagenesis, minor compactional porosity-loss and no mesogenetic changes because of burial to less than 2,000 m and subsequent uplift. The sand-grade part of the Tarporey Siltstones can be used as similar analogue but where there has been locally intense eogenetic growth of evaporite minerals.

The Lower Triassic sediments observed at Formby outcrop extensively across Great Britain and represent important aquifers and oil and gas reservoirs (Woodcock, 1993). Lower Triassic sediments (particularly Sherwood Sandstone Group deposits) have attracted renewed attention as part of the energy transition including for geothermal energy and carbon sequestration (Armitage et al., 2016, 2013; Downing et al., 1984; Gluyas et al., 2018; Hirst et al., 2015). Sherwood Sandstone Group (Ormskirk Sandstone Formation) sediments, sealed with significant thicknesses of overlying Mercia Mudstone Group sediments, could prove vital if carbon sequestration continues to grow within the United Kingdom (Armitage et al., 2016, 2013; Kirk, 2005). The UK's only current producing geothermal borehole is located near

Southampton; it extracts water from Sherwood Sandstone Group sediments, at a depth of just 1800 m below sea level (Gluyas et al., 2018). In contrast, Middle Triassic Tarporley Siltstone Formation deposits are typically overlooked or treated as 'waste zones' (Meadows et al., 1997) even though these rocks can have greater than 20 % porosity and 100 mD permeability (Figs. 10, 19-22). It may be appropriate to consider these lower Mercia Mudstone Group deposits as part of the reservoir system and not just part of the top-seal.

## 6 Conclusions

1. The stratigraphy present in the well Formby MFA-1 includes the Lower Triassic Ormskirk Sandstone Formation (known locally as the Helsby Sandstone Formation) from the Sherwood Sandstone Group, and the Middle Triassic Tarporley Siltstone Formation (known locally as the Keuper Waterstones Formation) from the Mercia Mudstone Group.
2. The Ormskirk Sandstone Formation is a medium grained sandstone. The Tarporley Siltstone Formation is comprised of interbedded evaporitic mudstone, siltstone and very fine sandstone.
3. The Triassic clastic sediments at Formby were deposited in intracontinental environments. The Ormskirk Sandstone Formation was deposited in a continental sabkha environment, comprised of deserts and ephemeral rivers. The Tarporley Siltstone Formation was deposited on the margins of a playa lake, with transient evaporitic conditions as a function of lake level.
4. The porosity and the permeability of the Ormskirk Sandstone Formation (17 to 32 % porosity and 200 to 9,000 mD permeability) are substantially higher than the Tarporley Siltstone Formation (8 to 20 % porosity and <0.01 to 110 mD permeability).

5. The main controls on reservoir quality differ substantially between the Ormskirk Sandstone Formation and Tarporley Siltstone Formation intervals. In the Ormskirk Sandstone Formation reservoir, porosity and permeability are controlled by primary grain size and sorting and variable degrees of compaction, with a minor control exerted by the quantities of carbonate and detrital clay minerals. For the Tarporley Siltstone Formation, reservoir quality is significantly lower than in the Ormskirk Sandstone Formation due to a combination of finer grain size, bed-controlled detrital clay matrix abundance and the presence of eogenetic pore-filling gypsum and carbonate cement.
6. The high intergranular porosity of the Ormskirk Sandstone Formation suggests relatively low degrees of compaction. The lack of any mesogenetic mineral cements, in both the Ormskirk Sandstone Formation and Tarporley Siltstone Formation, suggests that the reservoir at Formby has not been buried greater than about 1,000 to 1,500 m.
7. The reservoir at Formby can be used as an analogue for subsurface intervals planned for carbon capture and storage (offshore, East Irish Sea Basin) and geothermal energy provision (onshore, Cheshire Basin).

## Figure captions

Figure 1. a) Regional location map of the eastern East Irish Sea Basin. b) Major structural trends of the eastern East Irish Sea Basin (after Jackson and Mulholland, 1993). The extent of the regional cross section in Fig. 2. is indicated by A - A'.

Figure 2. Local location map of the Formby Oil Field. Selected historic exploration wells and structural elements are also indicated in the area. The regional location of Fig. 2 is indicated on Fig. 1b.

Figure 3. Generalised vertical section of Triassic sediments observed in the eastern East Irish Sea Basin (after Haig et al., 1997).

Figure 4. Regional cross section of the eastern East Irish Sea basin, showing the main structural elements present. The extent of the cross section is indicated on the Figure 1b. A - A'. The transition from the East Irish Sea Basin (EISB) to the West Lancashire Basin is indicated by the Formby Point Fault. The Formby Point Fault is a syn-sedimentary fault that trends NE, with thicker sediments observed basinward towards the EISB (after Yaloz and McKim, 2003).

Figure 5. Local cross section of the stratigraphy observed at the Formby Oilfield. The extent of the cross section is indicated on Fig. 2 B - B'. The Formby Oilfield is bound between the Hill House Fault and ?Ince Blundell Faults that trend NW-SE. Reservoir deposits are found within the Tarporley Siltstone Formation (part of the Mercia Mudstone Group) and the Ormskirk Sandstone Group Formation (part of the Sherwood Sandstone Group) (after Roche and Openshaw, 2011).

Figure 6. Original wireline log data for the Mesozoic part of the borehole (i.e., excluding the Quaternary). (a) Borehole diameter revealed by the caliper log revealing several intervals where the borehole is a lot wider than mean. (b) Gamma ray log revealing the abundance of radioactive minerals (mainly K-feldspar, micas and illite). (c) Density log (RHOB, solid grey line) and the neutron log NPHI, dashed black line); where the density log lies to the left of the neutron log, the crossover region is marked in pale yellow, representing net pay; the opposite regions are marked in brown representing non-net intervals. (d) The deep resistivity log, here

plotted on a log-scale; the steady decrease in resistivity through the thick zone of net pay represents an oil-water transition zone.

Figure 7. Interpreted wireline log data for the Mesozoic part of the borehole. (A) Interpreted shale abundance ( $V_{\text{shale}}$ ) with different baselines (minimum gamma) assumed for the Ormskirk Sandstone Formation and Tarporley Siltstone Formation (justified by the much greater feldspar concentration in the Tarporley than the Sherwood, see Appendix 4) with shading representing the shale content. The  $V_{\text{shale}}$  calculation assumes that all clay minerals are radioactive, or that the clays are wholly represented by the amount of illite (B) Comparison of  $N_{\text{shale}}$  (derived from the normalised difference between the neutron log and density-derived porosity) and  $V_{\text{shale}}$ .  $N_{\text{shale}}$  represents the sum total of all clays, not just radioactive clay, but it also represents H-mineral evaporite minerals such as gypsum. In this Mesozoic section, the difference in  $N_{\text{shale}}$  and  $V_{\text{shale}}$  reflects the greater quantity of chlorite in the Tarporley than the Ormskirk but it also probably represents the locally high concentration of gypsum in the Tarporley. (C) Synthetic (composite) log with porosity (from the density log), fluid types, (derived from the Archie equation) and lithology here simply split between sand and shale (based on the  $V_{\text{shale}}$  calculation). Core porosity data are also plotted to reveal the high degree of agreement between the log porosity and core porosity. The oil-water transition zone is evident below about 90 m. The thin-bedded pay zones from the Tarporley, with high oil saturation, are evident in the upper part of the section.

Figure 8. Interpreted wireline log data with density log-derived porosity plotted versus depth with data differentiated by  $V_{\text{shale}}$  (symbol size) and  $N_{\text{shale}}$  derived using the equation 5 (rainbow spectrum). The figure reveals that the Ormskirk is dominated by high porosity, low  $V_{\text{shale}}$  and low  $N_{\text{shale}}$  sandstones. It also confirms that the Tarporley is dominated by low

porosity, high  $V_{shale}$  and high  $N_{shale}$  rocks with up to six discrete beds of higher porosity and intermediate  $V_{shale}$ . The best reservoir quality rocks in the Tarporley have relatively high  $N_{shale}$  suggesting the presence of either non-radioactive clay minerals or gypsum.

Figure 9. Simplified sedimentary log of the Ormskirk Sandstone Formation (69.2 m to 94.23 m) stratigraphy present at Formby. Also displayed are core analysis porosity and permeability taken from core plugs and SEM-EDS of selected samples within the section. Key to facies codes: FL fluvial facies, AD aeolian dune facies, SS sand-sheet facies, SF sand-flat facies.

Figure 10. Simplified sedimentary log of the Tarporley Siltstone Formation (24.8 m to 69.2 m) stratigraphy present at Formby. Also displayed are core analysis porosity and permeability taken from core plugs and SEM-EDS of selected samples within the section. See Figure 9. for key to symbols in the sedimentary log. Key to facies codes: PL playa lake facies, SH sheet flood facies.

Figure 11: Core box photographs of selected sections from the Ormskirk Sandstone Formation (A and B) and Tarporley Siltstone Formation (C and D). (A) Sand flat facies of moderate reservoir quality from the Ormskirk Sandstone Formation (B) Aeolian dune facies of excellent reservoir quality within the Sherwood Sandstone Group, with grain-fall flow laminae present. (C) Playa lake facies of pore reservoir quality from the Tarporley Siltstone Formation, with a visible desiccation crack present. (D). Sheet flood facies of moderate reservoir quality from the Tarporley Siltstone Formation. Residual oil is visible in A, B and C.

Figure 12. Thin section optical micrographs and QEMSCAN<sup>®</sup> SEM-EDS images showing the key diagenetic and sedimentary features in the Ormskirk Sandstone Formation (Sherwood Sandstone Group) at Formby MFA-1. (A) (Sample 10, 73.02 m) Optical micrograph of a well sorted quartz arenite, containing phytophreatic dolocrete clasts. Fractures present are

artifacts from thin sectioning process. (B) (Sample 9, 70.91 m) SEM-EDS image of a well sorted feldspathic arenite, containing a phytophreatic dolocrete clast. (C) (Sample 13, 79.04 m) Optical micrograph of a well sorted sub-lithic arenite, with phytophreatic dolocrete clasts and muscovite mica present, some minor authigenic dolomite rhombs are also present. Grain dissolution of unstable feldspars are also observed, along with a thick residual oil coating and some minor grain coating detrital clays. (D) (Sample 20, 92.63m) SEM-EDS image of a well sorted sub-lithic arenite, highlighting finer laminae present. In finer bands increased feldspar grains and phytophreatic dolocrete clasts are observed. (E) (Sample 12, 76.56 m) Optical micrograph of a sub-lithic arenite, with observed pyrite present and second cycle quartz overgrowths present. (F) (Sample 15, 82.56 m). An SEM-EDS of a lithic arenite, highlighting feldspar dissolution creating secondary pore space. Lithics and dolomite cements are also found to be present. (G) (Sample 20, 92.63) Optical micrograph of a well sorted sub-lithic arenite, with volcanic lithics being observed. Grain dissolution is also observed creating both secondary isolated pore space and secondary connected pore space. (H) (Sample 14, 80.50 m) An SEM-EDS image of a sub-lithic arenite containing volcanic lithic grains and dolomite cements.

Figure 13. QFL lithofacies diagram based on point count data, quartz, feldspar and lithic fragments (including: micas, heavy mineral grains, sedimentary, metamorphic and igneous rock fragments). The Tarporley Siltstone Formation facies (playa and sheetflood) are distinctly more feldspathic than the Ormskirk Sandstone Formation facies, possibly reflecting a difference in provenance of the sediment. Figure 14. Thin section micrographs and QEMSCAN<sup>®</sup> SEM-EDS images showing the key diagenetic and sedimentary features in the Tarporley Siltstone Formation (Mercia Mudstone Group) at Formby MFA-1. (A) (Sample 2, 35.70 m) Optical micrograph of a well sorted feldspathic arenite containing muscovite and biotite mica



ductile grains, cemented by pervasive gypsum cement. (B) (Sample 1, 33.00 m) SEM-EDS image of a well feldspathic arenite with localised dolomite cement and pervasive gypsum cement. (C) (Sample 3, 38.92 m) Optical micrograph of a feldspathic arenite, authigenic pyrite and residual oil emplacement is observed. (D) (Sample 3, 38.92 m) SEM-EDS image of a feldspathic arenite. Early dolomite and calcite cements are observed, along with calcrete nodules. Later gypsum has pervasively filled remaining pore spaces. Heavy minerals are present in trace amounts, notably rutile. Thin carbonate cemented laminae are also observed. (E) (Sample 5, 43.65 m) Optical micrograph of a feldspathic arenite that contains minor primary porosity. Aligned ductile grains (muscovite and biotite) are present, with some muscovite being expanded and deformed. Fine carbonate cement is present, along with minor pyrite and grain dissolution. Some second cycle quartz overgrowths can also be observed. (F) (Sample 5, 43.65 m) an SEM-EDS image of a feldspathic arenite, showing compacted quartz grains. Ductile muscovite and biotite micas are present, along with minor feldspar dissolution. Later authigenic calcite and ferroan dolomite cements are also present. (G) (Sample 6, 49.59 m) Optical micrograph of a feldspathic arenite, with primary pore space filled by detrital clay and pyrite cement. Some ductile muscovite micas are also present, but not aligned. (H) (Sample 6, 49.59 m) SEM-EDS image of a feldspathic arenite, illustrating mica rich (biotite) detrital clay (laminae) present cemented by fine dolomite cements. Calcite cements can be found in areas of coarser grains.

Figure 15. A. Schematic facies model of Lower Triassic sediments of the Ormskirk Sandstone Formation (Sherwood Sandstone Group) around the Formby area. In the area around the North West of England (eastern East Irish Sea Basin, West Lancashire Basin and the Cheshire Basin), during the Lower Triassic sediments are fluvial-aeolian, sourced from mountainous upland areas (likely from alluvial fan feeders). B. Schematic facies model of the Middle to

Upper Triassic sediments of the Tarporley Siltstone Formation (Mercia Mudstone Group) in the area around the North West of England (eastern East Irish Sea Basin and West Lancashire Basin). During the Middle to Upper Triassic, sediment provenance is interpreted to have switched to a different fluvial-aolian source. Evaporitic and playa shales are likely to have been deposited during times of flood, with hinterland regions seeing sandflat deposits and areas of dune fields present. The local environments present at Formby (West Lancashire Basin) are indicated by the dashed red boxes; A. Ormskirk Sandstone Formation, B. Tarporley Siltstone Formation (modified after Goldsmith et al. 2003).

Figure 16. Schematic diagram of the main diagenetic events observed in the Ormskirk Sandstone Formation sediments at Formby. Early diagenetic cements are composed of early ferroan dolomite rhombs. Later diagenesis sees the widespread dissolution of unstable framework grains, mainly volcanic lithic fragments and feldspar grains. Minor pyrite can also be observed filling primary pore space prior to oil emplacement.

Figure 17. Schematic diagram of the main diagenetic events observed in the Tarporley Siltstone Formation sediments at Formby. Early diagenetic phases are composed of early carbonate cements (ferroan dolomite and calcite), followed by gypsum. Later diagenesis sees the dissolution of unstable framework grains (feldspar and minor volcanic grains). Precipitation of feldspar cements are common in later diagenesis in the form of intra and overgrowths. Late pyrite can be observed filling primary pore space prior to oil emplacement.

Figure 18. Intergranular volume (%) versus cement (%). Calculation of Compactional Porosity Loss (COPL) and Cementational Porosity Loss (CEPL), and the comparison diagram based on Houseknecht, (1987), based on petrographic data (including porosity), illustrating dominant porosity-loss processes for the Ormskirk Sandstone Formation and the Tarporley Siltstone

Formation. The Ormskirk is entirely dominated by compactional porosity-loss. The Tarporley has some samples dominated by cementation porosity-loss (these are gypsum cemented) but some are dominated by compaction.

Figure 19. Comparison of core analysis porosity and permeability data, differentiated by stratigraphy and the different ways to derive shale content using log data. (A)  $V_{shale}$ , using different base lines for the Ormskirk Sandstone Formation and the Tarporley Siltstone Formation, has a distinct effect on permeability, especially for the Ormskirk samples, with lower  $V_{shale}$  resulting in higher permeability. (B)  $N_{shale}$  (derived from the normalised difference between the neutron log and density-derived porosity) represents the sum total of all clays, not just radioactive clay, but it also represents H-mineral evaporite minerals such as gypsum. The higher total clay and gypsum concentration in the Tarporley than the Ormskirk is evident.

Figure 20. Comparison of core analysis porosity and permeability data differentiated by stratigraphy, lithofacies and texture. (A) Core analysis data split by depositional environment (Figs. 9 and 10); in contrast to assumptions made in many reservoir quality studies, depositional environment is not a good predictor of reservoir quality for either the Ormskirk or Tarporley Formations. (B) Core analysis data differentiated by texture and stratigraphy, using sorting defined by the phi-scale, where low number are very well sorted, higher numbers are less well-sorted. Grain size has a well-defined control on porosity and permeability but it is also evident that the degree of sorting has a major effect on permeability in the Ormskirk Sandstone Formation samples; for a similar grain size, porosity and permeability increase as sorting improves.

Figure 21. Comparison of core analysis porosity to relative compactional porosity loss (COPL) derived using the derived intergranular volume (sum of pore-filling cements and visible porosity) and the approach defined by Houseknecht (1987). The data have been split between the Ormskirk Sandstone Formation and the Tarporley Siltstone Formation subdivided into matrix-rich, gypsum-rich and other samples. The figure reveals that the range of core analysis porosity in the matrix- and early-cement-free sandstones is controlled by different degrees of compactional porosity-loss.

Figure 22. Core analysis permeability versus petrographically-defined sum total of authigenic mineral and matrix, with data differentiated by stratigraphy, grain size and sorting. The Tarporley Siltstone Formation has lower reservoir quality than the Ormskirk Sandstone Formation because they are finer-grained and have more cement than the Ormskirk. Permeability in the Ormskirk is significantly controlled by the amount of authigenic minerals but sorting and grain size also play a role with finer grained or more poorly sorted sandstones having lower permeability than coarser grained, better sorted sandstones. In essence, Tarporley reservoir quality is dominated by the quantity of authigenic minerals.

## **Table captions**

Table 1. Summary of facies descriptions and main bedding structures.

Table 2. Summary comparison of the main reservoir quality controls in the Ormskirk Sandstone Formation and Tarporley Siltstone Formation.

## **Appendix**

Appendix 1A. Tarporley Siltstone Formation, routine core analysis results from the Formby-MFA 1 well analysed by ALS Petrophysics.

Appendix 1B. Ormskirk Sandstone Formation, routine core analysis results from the Formby-MFA 1 well analysed by ALS Petrophysics.

Appendix 2: Point count data table.

Appendix 3. Table of sample numbers and depths studied in Formby MFA-1 and associated grain size data. Grain size data were acquired from averaging the measured long axis from 100 grains.

Appendix 4. SEM-EDS normalised data for analysed core plugs in the Formby MFA-1 well. Mineralogical data have been normalised to 100%. Visual normalised porosity is also indicated.

## **Acknowledgements**

We would like to thank PetroStrat for allowing the use of equipment to point count the samples, in particular. We would like to thank Ben Ursinus and Thomas Gould for their advice during point counting. We would also like to thank Thermo-Fisher-FEI Company (Hillsboro, Oregon) for loan of the SEM-EDS QEMSCAN equipment and associated software and Dr Alan Butcher for offering excellent analytical and geological advice throughout the loan period of the QEMSCAN. Scott Parker and Francois Ollivier from ALS Core Store in Guildford are thanked

for being convivial hosts during core logging and sampling. Thanks to two reviewers for excellent and very supportive comments that have led to an improved paper.

## References Mendeley

Allen, D.J., Holloway, S., 1984. Investigation of the geothermal potential of the UK: The Wessex Basin. British Geological Survey London.

Ambrose, K., Hough, E., Smith, N.J.P., Warrington, G., 2014. Lithostratigraphy of the Sherwood Sandstone Group of England, Wales and south-west Scotland. Br. Geol. Surv. Res. Rep. RR/14/01 50.

Armitage, P.J., Faulkner, D.R., Worden, R.H., Aplin, A.C., Butcher, A.R., Iliffe, J., 2011. Experimental measurement of, and controls on, permeability and permeability anisotropy of caprocks from the CO<sub>2</sub> storage project at the Krechba Field, Algeria. J. Geophys. Res. Solid Earth 116.

Armitage, P.J., Worden, R.H., Faulkner, D.R., Aplin, A.C., Butcher, A.R., Espie, A.A., 2013. Mercia Mudstone Formation caprock to carbon capture and storage sites: petrology and petrophysical characteristics. J. Geol. Soc. London. 170, 119–132.

Armitage, P.J., Worden, R.H., Faulkner, D.R., Butcher, A.R., Espie, A.A., 2016. Permeability of the Mercia Mudstone: suitability as caprock to carbon capture and storage sites. Geofluids 16, 26–42.

Beard, D.C., Weyl, P.K., 1973. Influence of texture on porosity and permeability of unconsolidated sand. Am. Assoc. Pet. Geol. Bull. 57, 349–369.

Beaumont, E.A., Foster, N.H., Hartmann, D.J., Beaumont, E.A., 2019. Predicting Reservoir

System Quality and Performance, in: Exploring for Oil and Gas Traps.  
<https://doi.org/10.1306/trhbk624c9>

Binney, E.W., Talbot, J.H., 1869. On the petroleum found in the Downholland Moss near Ormskirk. *Trans. Manchester Geol. Soc.*

Bowman, M.B.J., McClure, N.M., Wilkinson, D.W., 1993. Wytch Farm oilfield: deterministic reservoir description of the Triassic Sherwood Sandstone, in: Geological Society, London, Petroleum Geology Conference Series. Geological Society of London, pp. 1513–1517.

Bunce, J., 2018. The history of exploration and development of the Liverpool Bay fields and the East Irish Sea Basin. *Geol. Soc. Spec. Publ.* 465, 95–118. Jonathan Craig, Francesco Gerali, Fiona Macaulay, Rasoul Sorkhabi. <https://doi.org/10.1144/SP465.6>

Burley, S.D., 1984. Patterns of diagenesis in the Sherwood Sandstone Group (Triassic), United Kingdom. *Clay Miner.* 19, 403–440.

Cade, C.A., Evans, I.J., Bryant, S.L., 1994. Analysis of permeability controls: a new approach. *Clay Miner.* 29, 491–501.

Cope, F.W., 1939. Oil Occurrences in South-West Lancashire. *Bull. Geol. Surv. Gt. Britain* 2, 18–25.

Cowan, G., Burley, S.D., Hoey, N., Holloway, P., Bermingham, P., Beveridge, N., Hamborg, M., Sylta, Ø., 1999. Oil and gas migration in the Sherwood Sandstone of the East Irish Sea Basin, in: *Petroleum Geology of Northwest Europe: Proceedings of the 5th Conference*. Geological Society, London, p. 1398.

Craig, J., Gerali, F., Macaulay, F., Sorkhabi, R., 2018. The history of the European oil and gas

industry (1600s-2000s). Geol. Soc. Spec. Publ. 465, 1–24.  
<https://doi.org/10.1144/SP465.23>

De Pater, C.J., Baisch, S., 2011. Geomechanical study of Bowland Shale seismicity (unpublished), Synthesis report, 02/11/2011. Cuadrilla Resources Ltd.  
<http://heskethbankcouncil.uk/wp-content/uploads/Articles/Bowland%20Final%20Report.pdf>.

Downing, R.A., Allen, D.J., Barker, J.A., Burgess, W.G., Gray, D.A., Price, M., Smith, I.F., 1984. Geothermal exploration at Southampton in the UK: a case study of a low enthalpy resource. *Energy Explor. Exploit.* 2, 327–342.

Earp, J.R., Taylor, B.J., 1986. *Geology of the country around Chester and Winsford*, Memoir 109. ed, British Geological Survey Memoirs Series.

Gluyas, J., Auld, A., Adams, C., Hirst, C., Hogg, S., Craig, J., 2018. Geothermal potential of the global oil industry. *InTechOpen*. <https://doi.org/10.5772/intechopen.81062>

Griffiths, J., Faulkner, D.R., Edwards, A.P., Worden, Richard H., 2018. Deformation band development as a function of intrinsic host-rock properties in Triassic Sherwood Sandstone. *Geol. Soc. Spec. Publ.* 435, 161–176P. J. Armitage, A. R. Butcher, J. M. Churchill, A. E. Csoma, C. Hollis, R. H. Lander, J. E. Omma, R. H. Worden.  
<https://doi.org/10.1144/SP435.11>

Haig, D.B., Pickering, S.C., Probert, R., 1997. The Lennox oil and gas Field. *Geol. Soc. Spec. Publ.* 124, 417–436N. S. Meadows, S. R. Trueblood, M. Hardman, G. Cowan.  
<https://doi.org/10.1144/GSL.SP.1997.124.01.25>

Hirst, C.M., Gluyas, J.G., Adams, C.A., Mathias, S.A., Bains, S., Styles, P., 2015. UK Low Enthalpy



Geothermal Resources: the Cheshire Basin, in: Proceedings World Geothermal Congress Melbourne, Australia.

Hogg, A.J.C., Mitchell, A.W., Young, S., 1996. Predicting well productivity from grain size analysis and logging while drilling. *Pet. Geosci.* 2, 1–15.

Holloway, S., 2009. Storage capacity and containment issues for carbon dioxide capture and geological storage on the UK continental shelf. *Proc. Inst. Mech. Eng. Part A J. Power Energy* 223, 239–248.

Holloway, S., Milodowski, A.E., Strong, G.E., Warrington, G., 1989. The Sherwood Sandstone Group (Triassic) of the Wessex Basin, southern England. *Proc. Geol. Assoc.* 100, 383–394.

Houseknecht, D.W., 1987. Assessing the relative importance of compaction processes and cementation to reduction of porosity in sandstones. *Am. Assoc. Pet. Geol. Bull.* 71, 633–642. <https://doi.org/10.1306/9488787f-1704-11d7-8645000102c1865d>

Howard, A.S., Warrington, G., Ambrose, K., Rees, J.G., 2008. A formational framework for the Mercia Mudstone Group (Triassic) of England and Wales. *Br. Geol. Surv. Res. Rep.* 41.

Jackson, D.I., Mulholland, P., 1993. Tectonic and stratigraphic aspects of the East Irish Sea Basin and adjacent areas: contrasts in their post-Carboniferous structural styles, in: Geological Society, London, Petroleum Geology Conference Series. Geological Society of London, pp. 791–808.

Jackson, D.I., Mulholland, P., Jones, S.M., Warrington, G., Brooks, J., Glennie, K., 1987. The geological framework of the East Irish Sea basin. Graham & Trotman Limited.

Jones, N.S., Ambrose, K., 1994. Triassic sandy braidplain and aeolian sedimentation in the

- Sherwood Sandstone Group of the Sellafield area, west Cumbria. *Proc. Yorksh. Geol. Soc.* 50, 61–76.
- Kent, P.E., 1948. A deep borehole at Formby, Lancashire. *Geol. Mag.* 85, 253–264.
- Kirk, K.L., 2005. Potential for storage of carbon dioxide in the rocks beneath the East Irish Sea, NERC, British Geological Survey (unpublished). (CR/05/127N).  
<http://nora.nerc.ac.uk/id/eprint/11300>.
- Leppard, B., 2012. Core description and sedimentology of Well Formby MFA-1 (unpublished). Fleet. Aurora Petroleum Limited, Leppard Sedimentology report no. 93/12 (October 2012).
- McKie, T., Aggett, J., Hogg, A.J.C., 1998. Reservoir architecture of the upper Sherwood Sandstone, Wytch Farm field, southern England. *Geol. Soc. Spec. Publ.* 133, 399–406  
John R Underhill. <https://doi.org/10.1144/GSL.SP.1998.133.01.21>
- Meadows, N.S., Beach, A., 1993. Controls on reservoir quality in the Triassic Sherwood Sandstone of the Irish Sea, in: Geological Society, London, Petroleum Geology Conference Series. Geological Society of London, pp. 823–833.
- Meadows, N.S., Hardman, M., Cowan, G., 1997. Petroleum geology of the Irish Sea and adjacent areas. Geological Society of London, London.
- Medici, G., West, L.J., Mountney, N.P., Welch, M., 2019. Permeability of rock discontinuities and faults in the Triassic Sherwood Sandstone Group (UK): insights for management of fluvio-aeolian aquifers worldwide. *Hydrogeol. J.* 27, 2835–2855.
- Minchin, D.J., McEvoy, F.M., Harrison, D.J., Cameron, D.G., Evans, D.J., Lott, G.K., Hobbs, S.F.,

- Highley, D.E., 2005. Mineral resource information in support of national, regional and local planning: Merseyside (comprising City of Liverpool and Boroughs of Knowlsey, Sefton, St. Helens and Wirral).
- Mohamed, E.A., Worden, R.H., 2006. Groundwater compartmentalisation: a water table height and geochemical analysis of the structural controls on the subdivision of a major aquifer, the Sherwood Sandstone, Merseyside, UK.
- Neufelder, R.J., Bowen, B.B., Lahann, R.W., Rupp, J.A., 2012. Lithologic, mineralogical, and petrophysical characteristics of the Eau Claire Formation: Complexities of a carbon storage system seal. *Lithologic, Mineralogical, and Petrophysical Characteristics, Eau Claire Formation. Environ. Geosci.* 19, 81–104.
- Newell, D.L., Kaszuba, J.P., Viswanathan, H.S., Pawar, R.J., Carpenter, T., 2008. Significance of carbonate buffers in natural waters reacting with supercritical CO<sub>2</sub>: Implications for monitoring, measuring and verification (MMV) of geologic carbon sequestration. *Geophys. Res. Lett.* 35.
- Pharaoh, T.C., Smith, N.J.P., Kirk, K., Kimbell, G.S., Gent, C., Quinn, M., Monaghan, A.A., 2016. Palaeozoic petroleum systems of the Irish Sea.
- Plummer, P.S., Gostin, V.A., 1981. Shrinkage cracks; desiccation or syneresis? *J. Sediment. Res.* 51, 1147–1156.
- Rider, M., Kennedy, M., 2011. The geological interpretation of well logs: Rider-French Consulting Limited.
- Roche, I.P., 2012. Lessons from history-unlocking a new UK shale oil play, in: SPE/EAGE European Unconventional Resources Conference & Exhibition-From Potential to

Production.

Roche, I.P., Openshaw, S.J., 2011. Exploration and Appraisal of Shallow Onshore Hydrocarbon Accumulations Using Resistivity Tomography, Formby Area, UK, in: 73rd EAGE Conference and Exhibition Incorporating SPE EUROPEC 2011.

Rowley, E., White, N., 1998. Inverse modelling of extension and denudation in the East Irish Sea and surrounding areas. *Earth Planet. Sci. Lett.* 161, 57–71.

Schmid, S., Worden, R.H., Fisher, Q.J., 2006. Sedimentary facies and the context of dolocrete in the Lower Triassic Sherwood Sandstone group: Corrib Field west of Ireland. *Sediment. Geol.* 187, 205–227.

Schmid, S., Worden, R.H., Fisher, Q.J., 2004. Diagenesis and reservoir quality of the Sherwood Sandstone (Triassic), Corrib field, Slyne basin, west of Ireland. *Mar. Pet. Geol.* 21, 299–315.

Schmid, S., Worden, R.H., Fisher, Q.J., 2003. The origin and regional distribution of dolomite cement in sandstones from a Triassic dry river system, Corrib Field, offshore west of Ireland. *J. Geochemical Explor.* 78, 475–479.

Seedhouse, J.K., Racey, A., 1997. Sealing capacity of the Mercia Mudstone Group in the East Irish Sea Basin: implications for petroleum exploration. *J. Pet. Geol.* 20, 261–286.

Shedid, S.A., Saad, M.A., 2017. Comparison and sensitivity analysis of water saturation models in shaly sandstone reservoirs using well logging data. *J. Pet. Sci. Eng.* 156, 536–545.  
<https://doi.org/10.1016/j.petrol.2017.06.005>

Spötl, C., Wright, V.P., 1992. Groundwater dolocretes from the Upper Triassic of the Paris

- Basin, France: a case study of an arid, continental diagenetic facies. *Sedimentology* 39, 1119–1136.
- Strong, G.E., 1993. Diagenesis of Triassic Sherwood Sandstone Group rocks, Preston, Lancashire, UK: A possible evaporitic cement precursor to secondary porosity? *Geol. Soc. Spec. Publ.* 73, 279–289C. P. North, D. J. Prosse. <https://doi.org/10.1144/GSL.SP.1993.073.01.17>
- Swann, G., Munns, J., 2003. The hydrocarbon prospectivity of Britain's onshore basins. DTI, London 17.
- Tiab, D., Donaldson, E.C., 2015. *Petrophysics: theory and practice of measuring reservoir rock and fluid transport properties*. Gulf professional publishing.
- Tunbridge, I.P., 1984. Facies model for a sandy ephemeral stream and clay playa complex; the Middle Devonian Trentishoe Formation of North Devon, UK. *Sedimentology* 31, 697–715.
- Woodcock, N., 1993. JCW Cope, JK Ingham & PF Rawson (eds) 1992. *Atlas of Palaeogeography and Lithofacies*. Geological Society Memoir no. 13. xi+ 155 pp. London, Bath: The Geological Society. Price£ 295.00 (hard covers). ISBN 0 903317 65 6. *Geol. Mag.* 130, 409–410.
- Wooldridge, L.J., Worden, R.H., Griffiths, J., Utley, J.E.P., Thompson, A., 2018. The origin of clay-coated sand grains and sediment heterogeneity in tidal flats. *Sediment. Geol.* 373, 191–209. <https://doi.org/https://doi.org/10.1016/j.sedgeo.2018.06.004>
- Worden, R.H., 1998. Dolomite cement distribution in a sandstone from core and wireline data: the Triassic fluvial Chaunoy Formation, Paris Basin. *Geol. Soc. Spec. Publ.* 136, 197–211P. K. Harvey, M. A. Lovell. <https://doi.org/10.1144/GSL.SP.1998.136.01.17>

- Worden, R.H., Armitage, P.J., Butcher, A.R., Churchill, J.M., Csoma, A.E., Hollis, C., Lander, R.H., Omma, J.E., 2018. Petroleum reservoir quality prediction: Overview and contrasting approaches from sandstone and carbonate communities. *Geol. Soc. Spec. Publ.* 435, 1–31. <https://doi.org/10.1144/SP435.21>
- Worden, R.H., Burley, S.D., 2003. Sandstone diagenesis: the evolution of sand to stone. *Sandstone Diagenes. Recent Anc.* 4, 3–44.
- Worden, R.H., Coleman, M.L., Matray, J.M., 1999. Basin scale evolution of formation waters: a diagenetic and formation water study of the Triassic Chaunoy Formation, Paris Basin. *Geochim. Cosmochim. Acta* 63, 2513–2528.
- Worden, R.H., Matray, J.M., 1998. Carbonate cement in the Triassic Chaunoy Formation of the Paris Basin: Distribution and effect on flow properties. *Carbonate Cem. sandstones Distrib. patterns geochemical Evol.* 163–177.
- Yaliz, A., Chapman, T., 2003. The Lennox Oil and Gas Field, Block 110/15, East Irish Sea. *Geol. Soc. London, Mem.* 20, 87–96.
- Yaliz, A., McKim, N., 2003. The Douglas Oil Fields, Block 110/13b, East Irish Sea. *Geol. Soc. London, Mem.* 20, 61–75. <https://doi.org/10.1144/GSL.MEM.2003.020.01.05>
- Yaliz, A., Taylor, P., 2003. The Hamilton and Hamilton North Gas Fields, Block 110/13a, East Irish Sea. *Geol. Soc. London, Mem.* 20, 77–86.
- Yaliz, A.M., 1997. The Douglas Oil Field. *Geol. Soc. Spec. Publ.* 124, 399–416N. S. Meadows, S. R. Trueblood, M Hardman, G. Cowan. <https://doi.org/10.1144/GSL.SP.1997.124.01.24>

Figure 1.

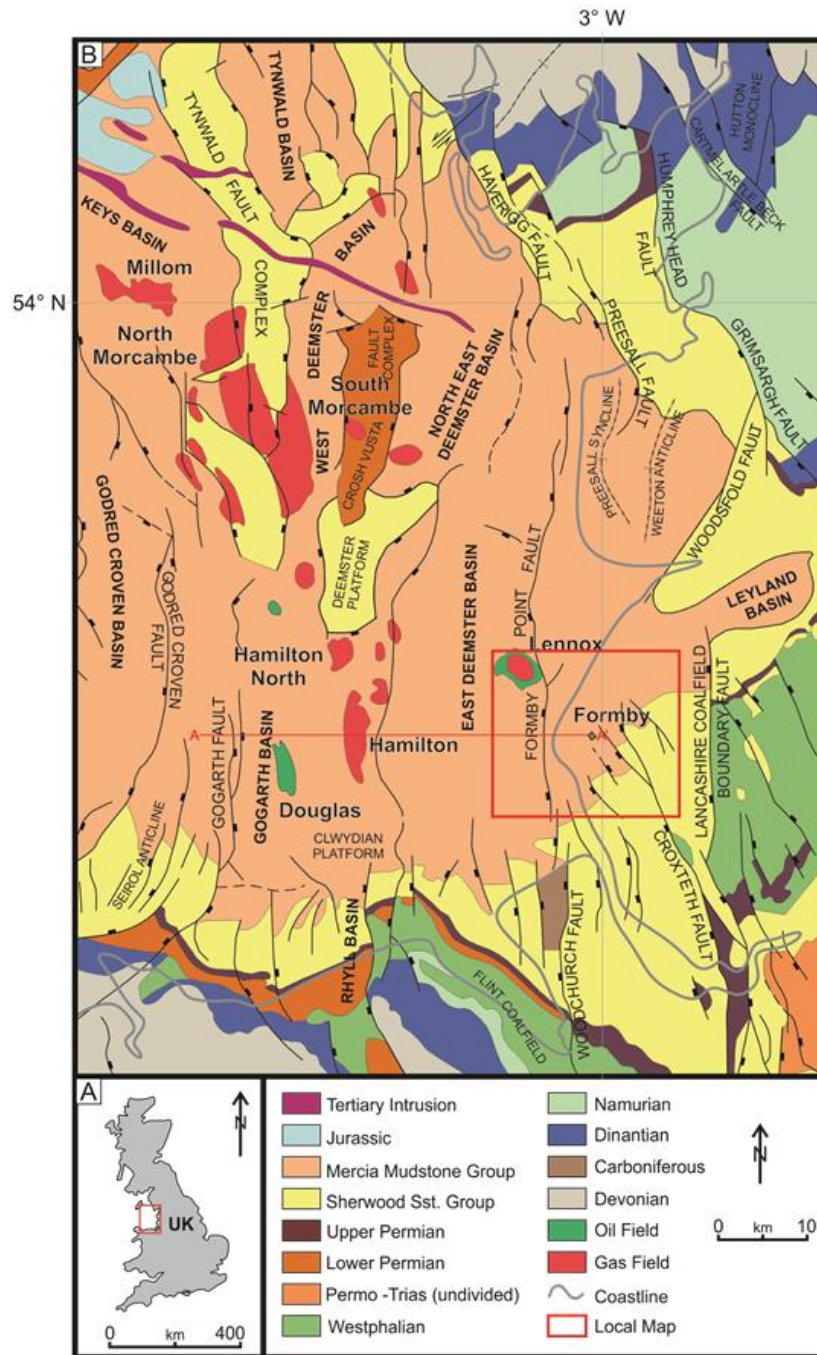


Figure 2.

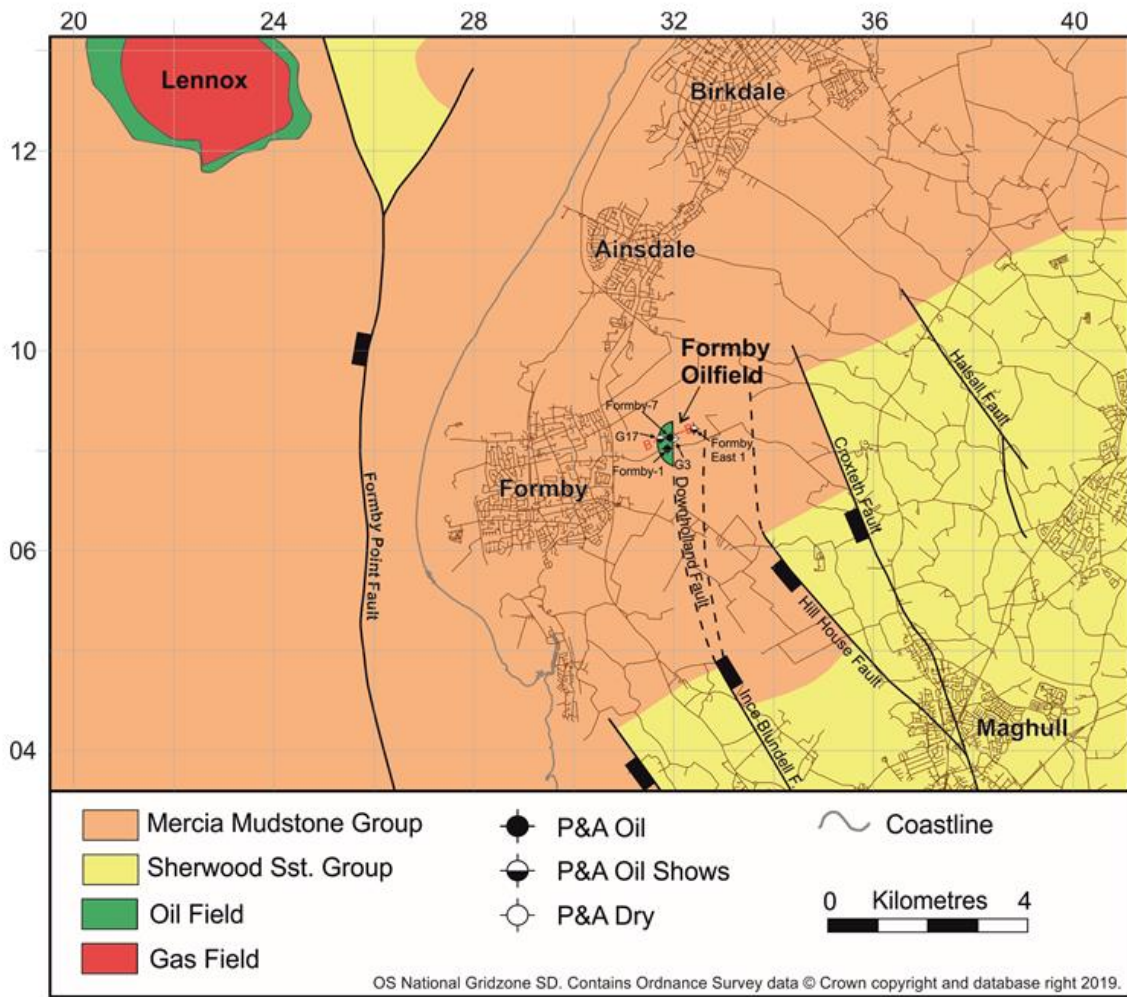




Figure 3.

Period	Epoch	Age	Principle Stratigraphic Groups	Irish Sea	Blackpool and The Fylde	Formby-7	Liverpool, Wirral and N. Cheshire	
Triassic	Late	Rhaetian	Penarth Group		... TOP, NOT SEEN ...			
		Norian	Mercia Mudstone Group	... TOP, NOT SEEN ... Unnamed Mudstone	Breckells Mudstone Formation		... TOP, NOT SEEN ...	
		Carnian		Wilkesley Halite Equivalent			Wilkesley Halite Formation	
	Ladinian	Unnamed Mudstone				Middle Marl Formation		
	Middle	Anisian		Preesall Halite Equivalent	Kirkham Mudstone Formation ↔ Preesall Halite	... TOP, NOT SEEN ...	Northwich Halite Formation	
				Unnamed Mudstone			Lower Marl Formation	
				Mythop Halite Equivalent	Singleton Mudstone Formation ↔ Mythop Halite		Tarporley Siltstone Formation	
				Unnamed Mudstone			Tarporley Siltstone Formation	
				Rossall Halite Equivalent	Hambledon Mudstone		Frodsham Mbr.	
	Early	Scythian	Sherwood Sandstone Group		Ormskirk Sandstone Formation	Ormskirk Sandstone Formation	Ormskirk Sandstone Formation (Helsby Sat Equ.)	Helsby Sat Fm.
				St Bees Sandstone Formation	St Bees Sandstone Formation	Wilslow Sandstone Formation		Wilslow Sandstone Formation
						Kinnerton Sandstone Formation		
							Delamere Mbr.	
							Thurstaston Mbr.	

Figure 4.

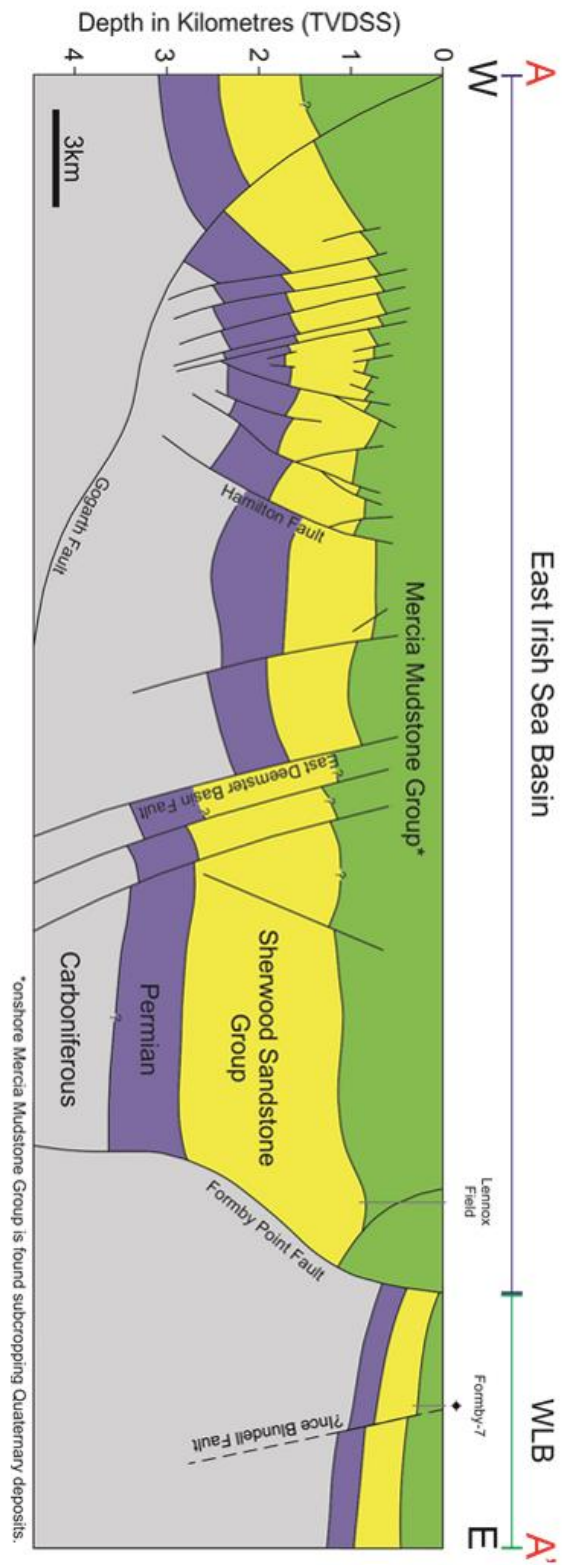


Figure 5.

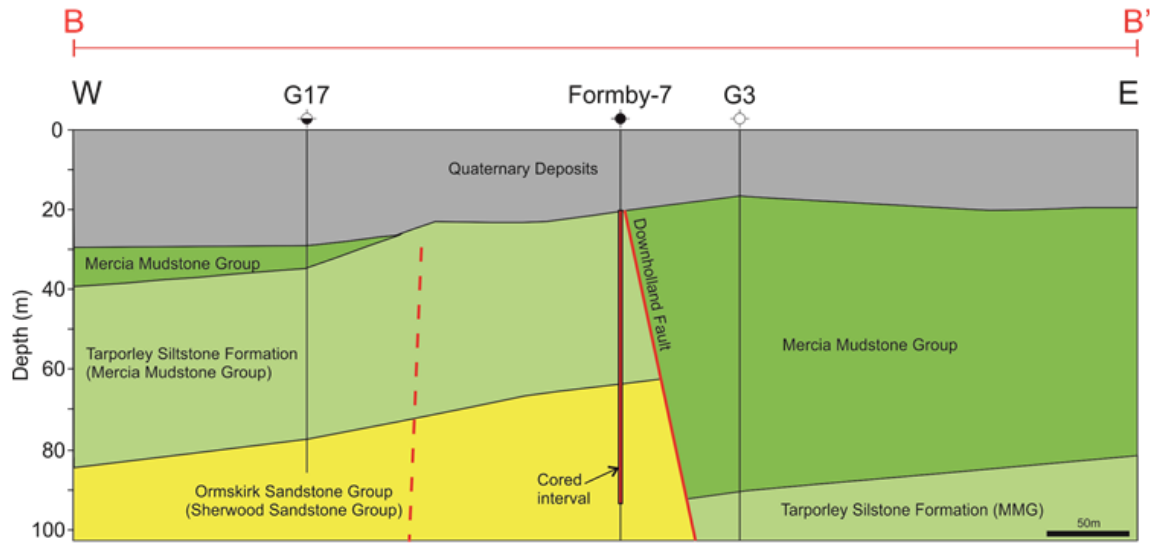


Figure 6.

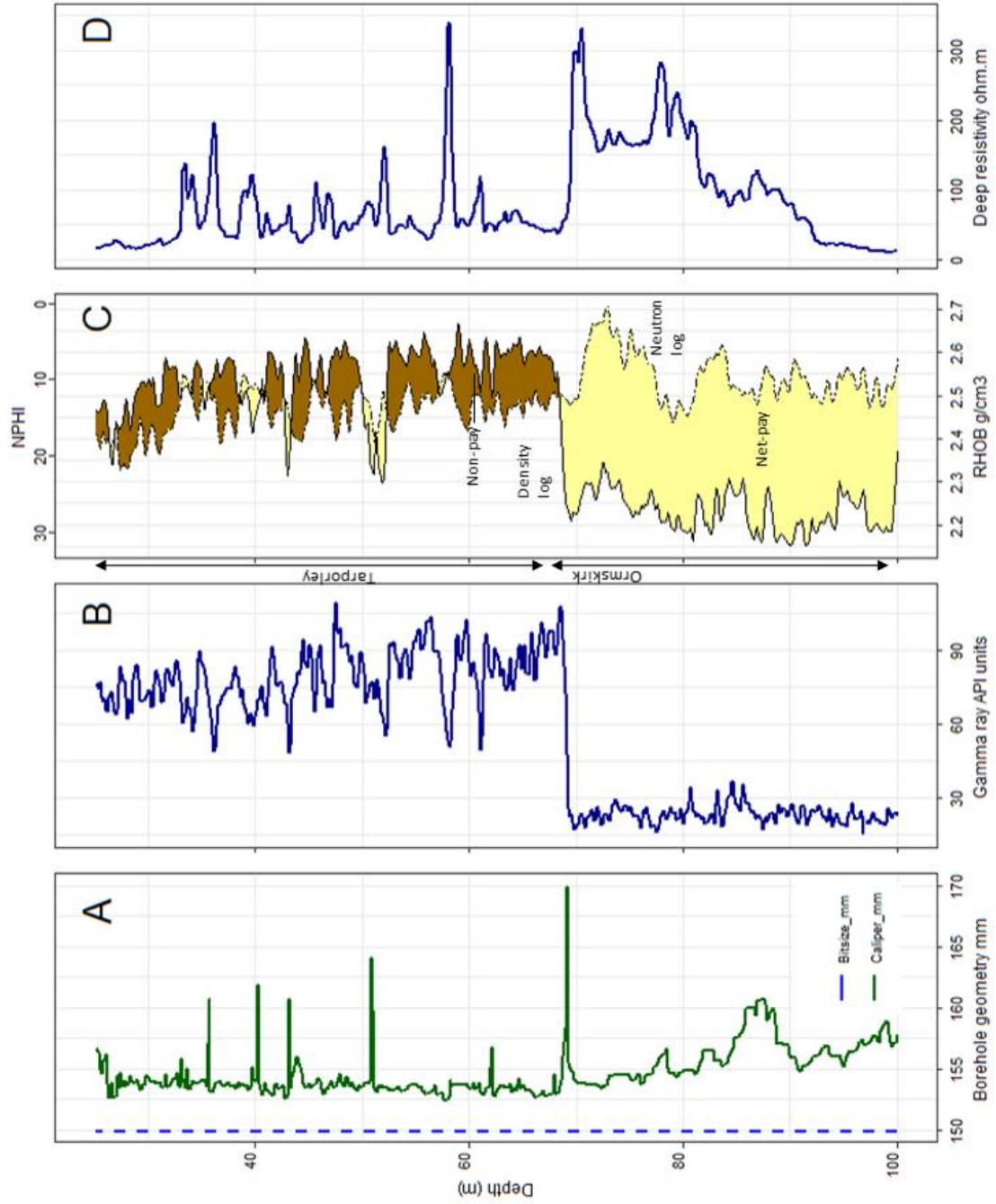


Figure 7.

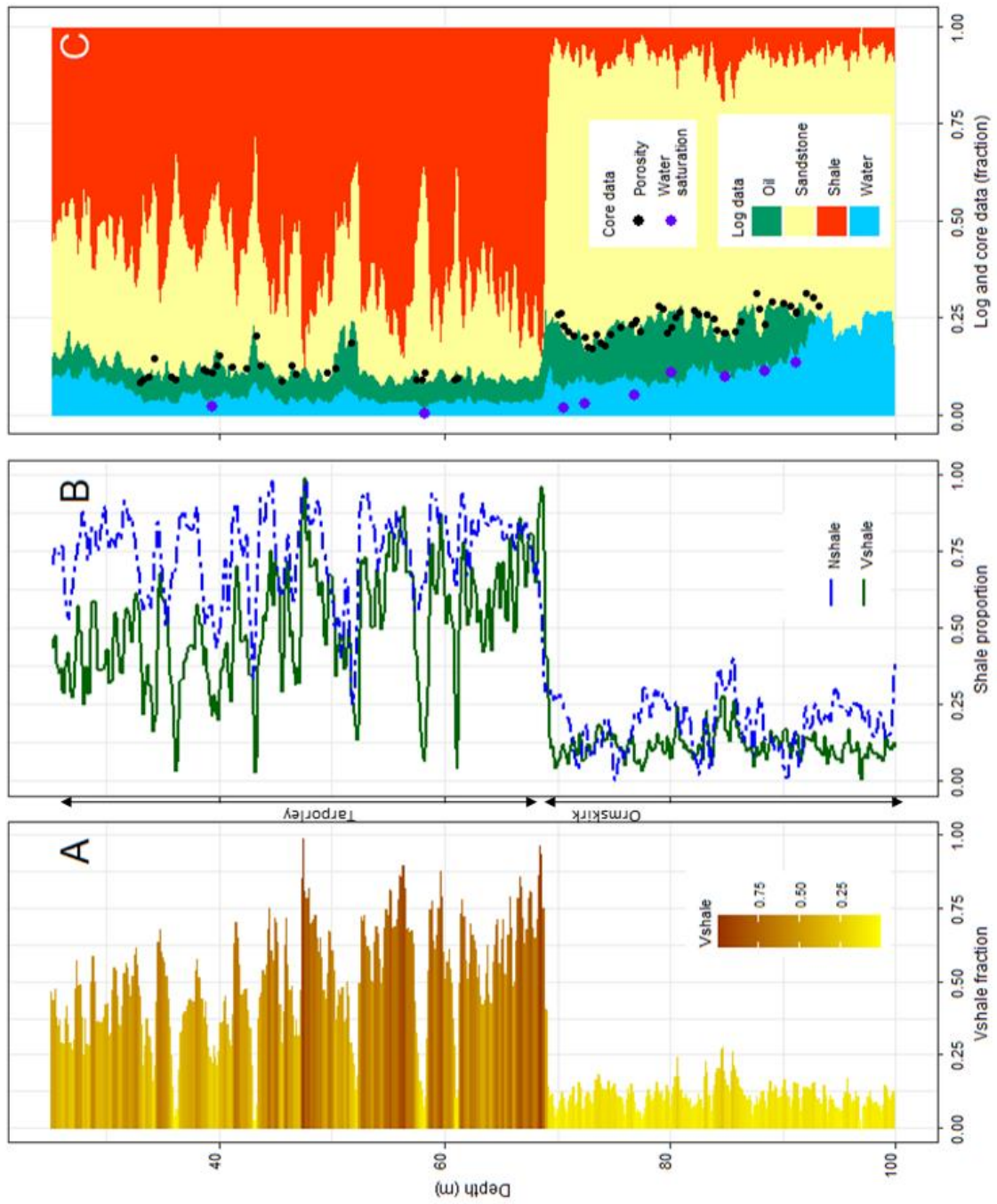


Figure 8.

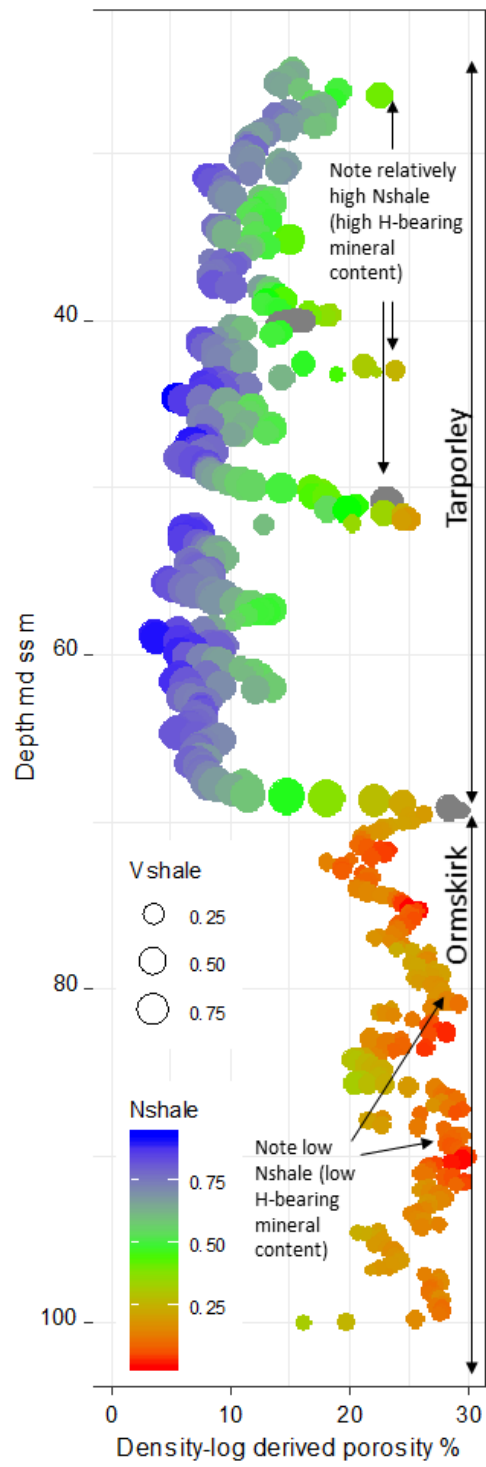


Figure 9.

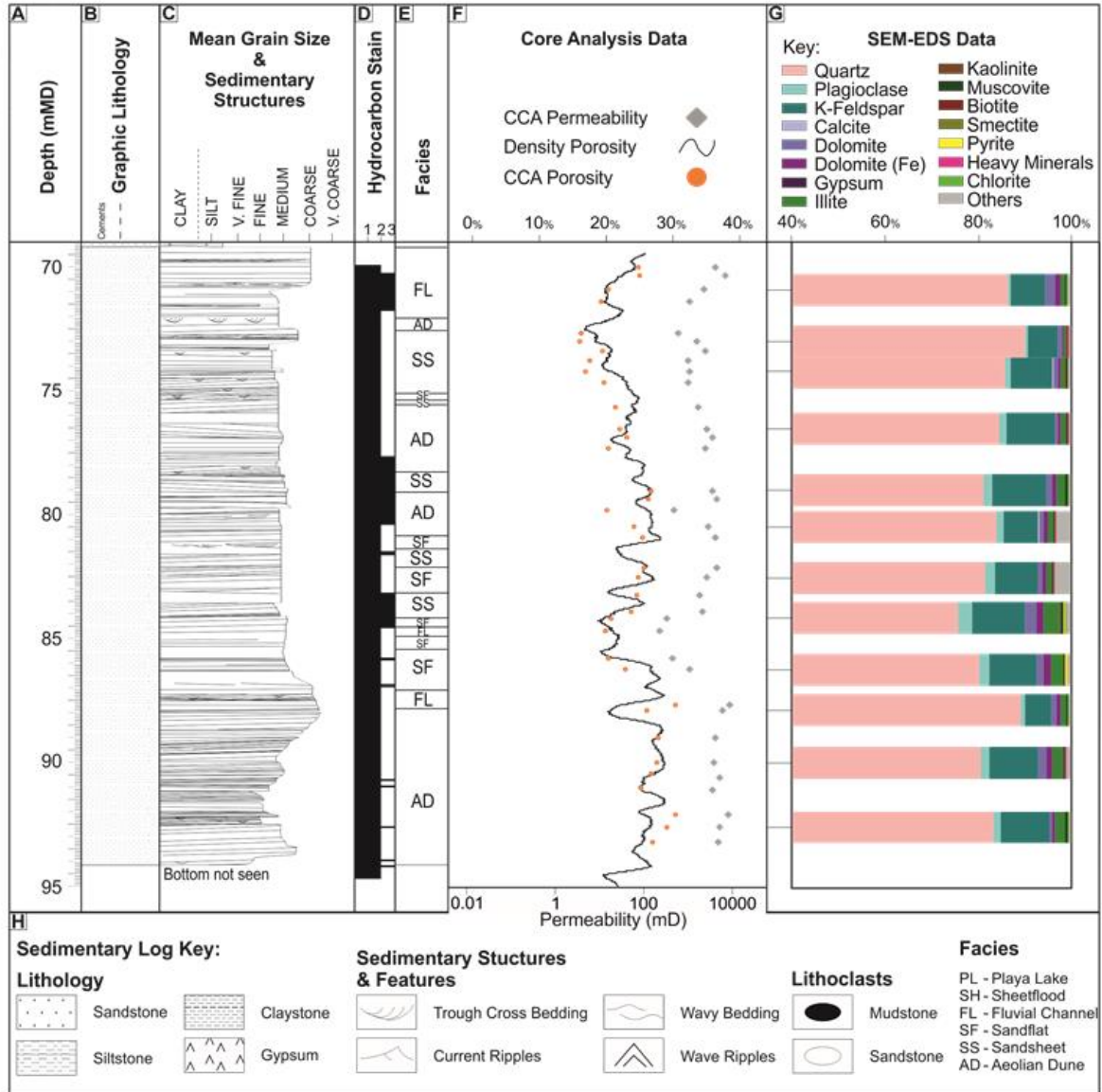


Figure 10.

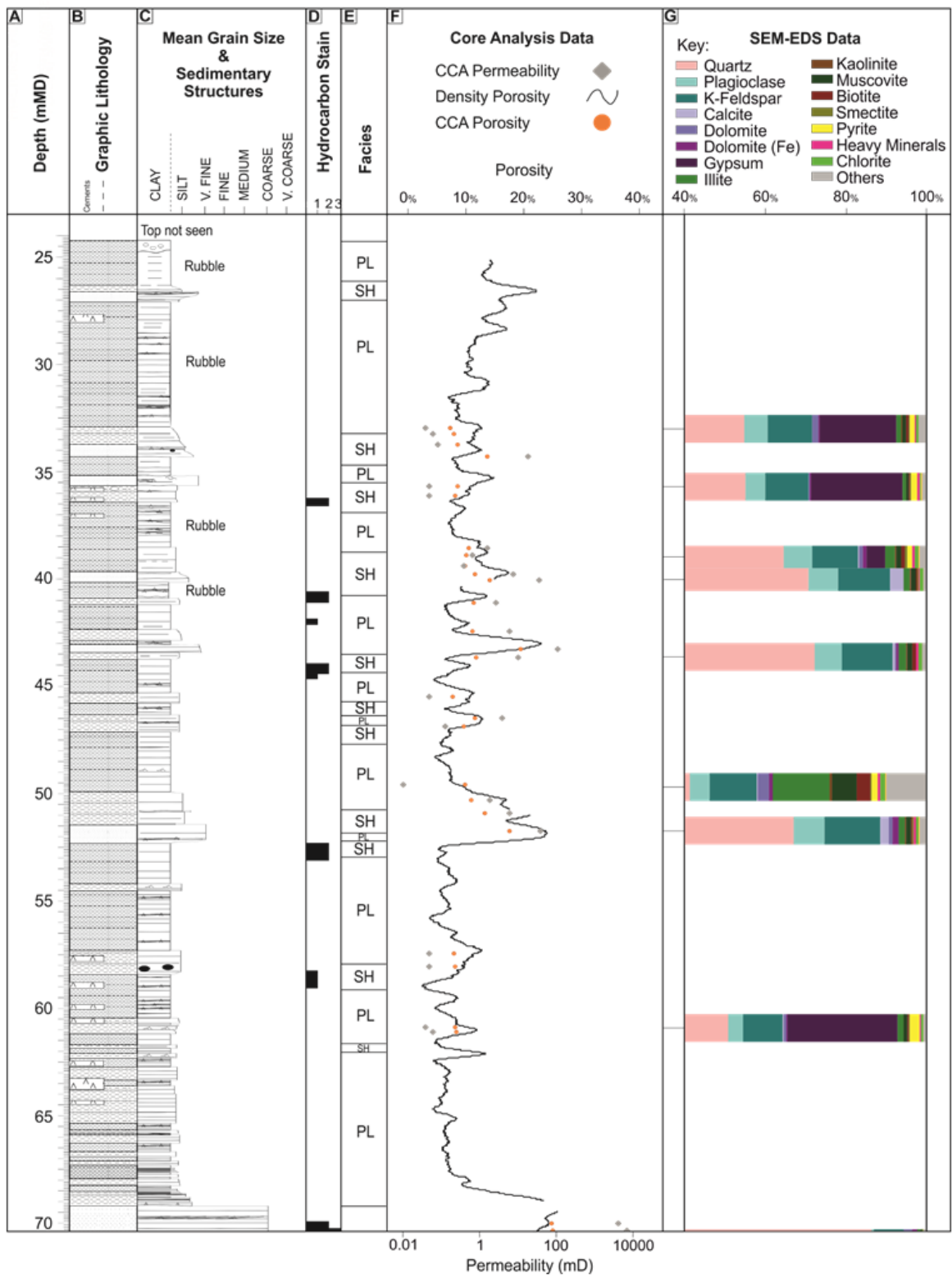




Figure 11.

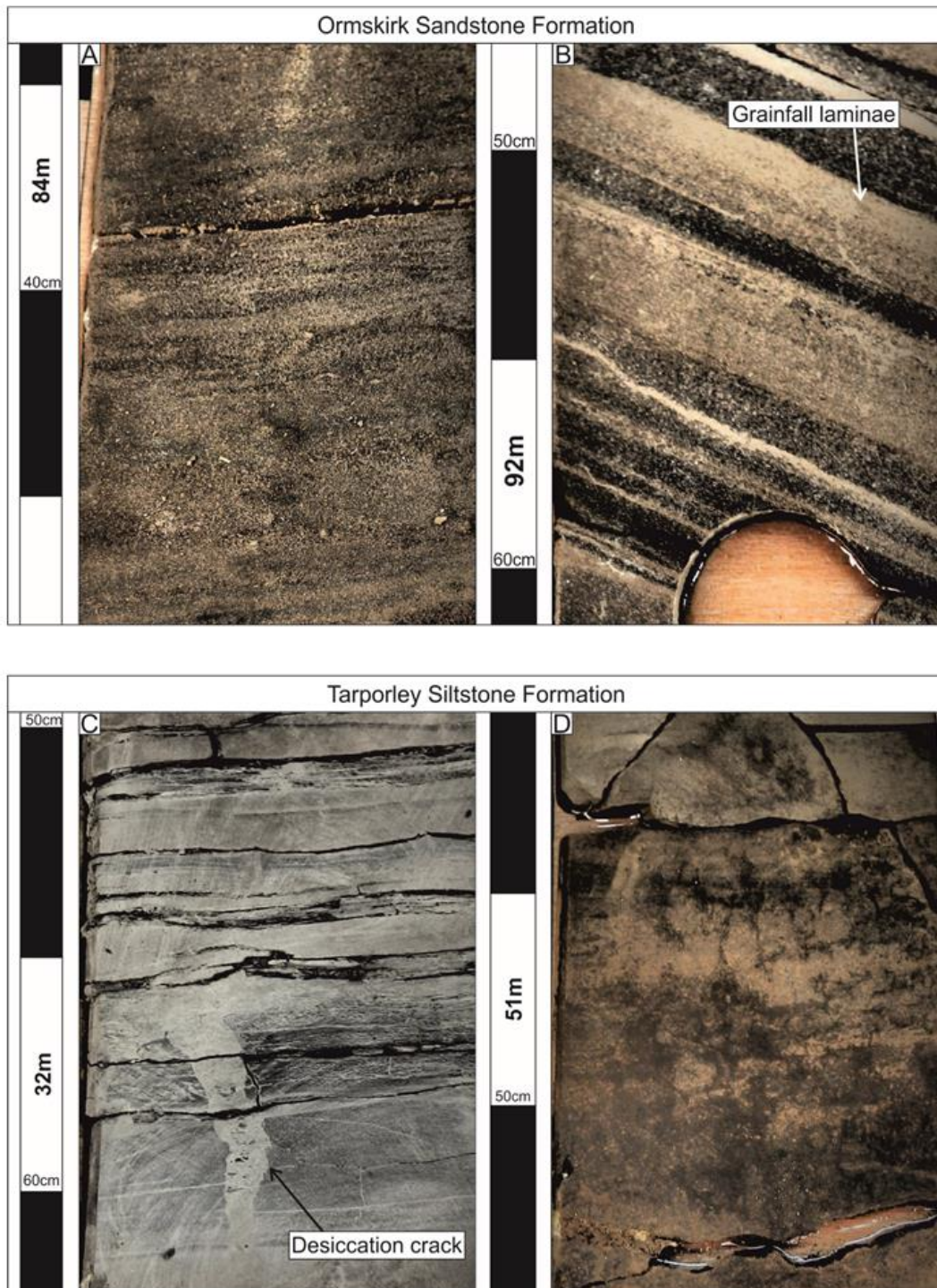


Figure 12.

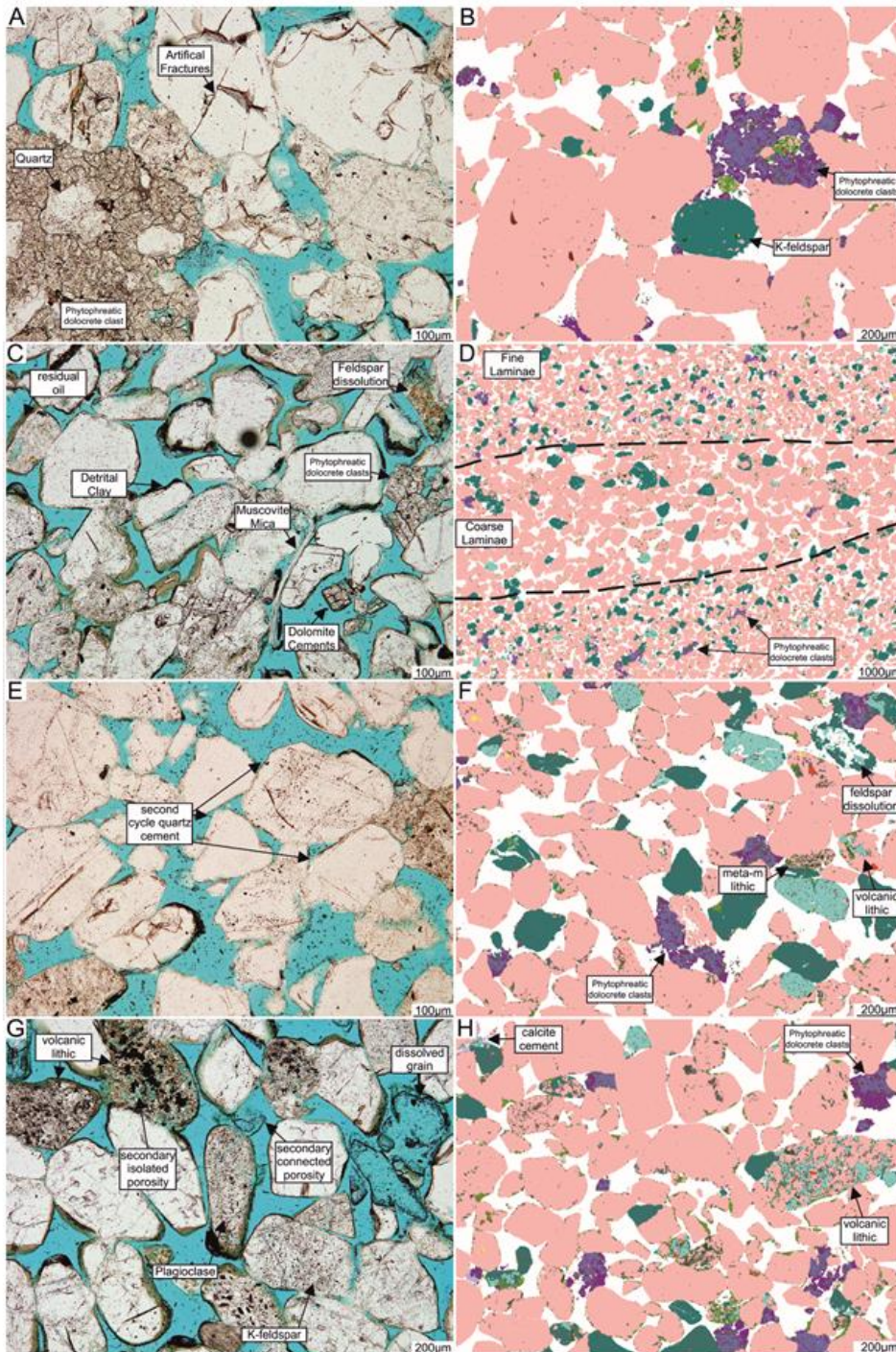


Figure 13

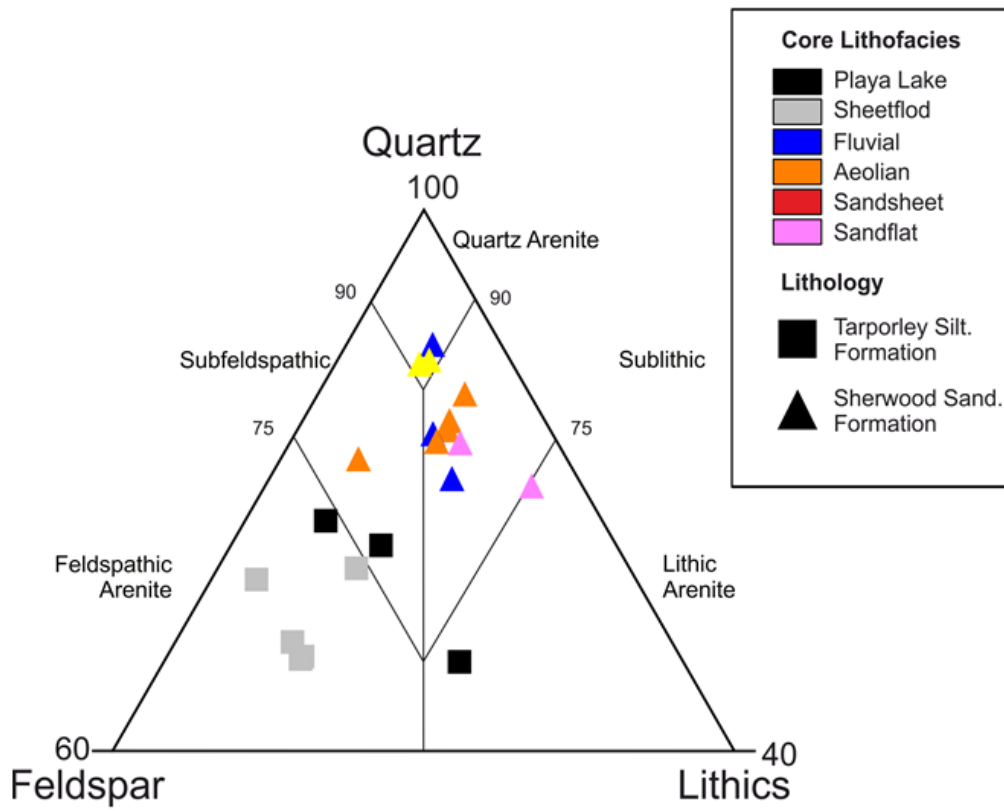


Figure 14

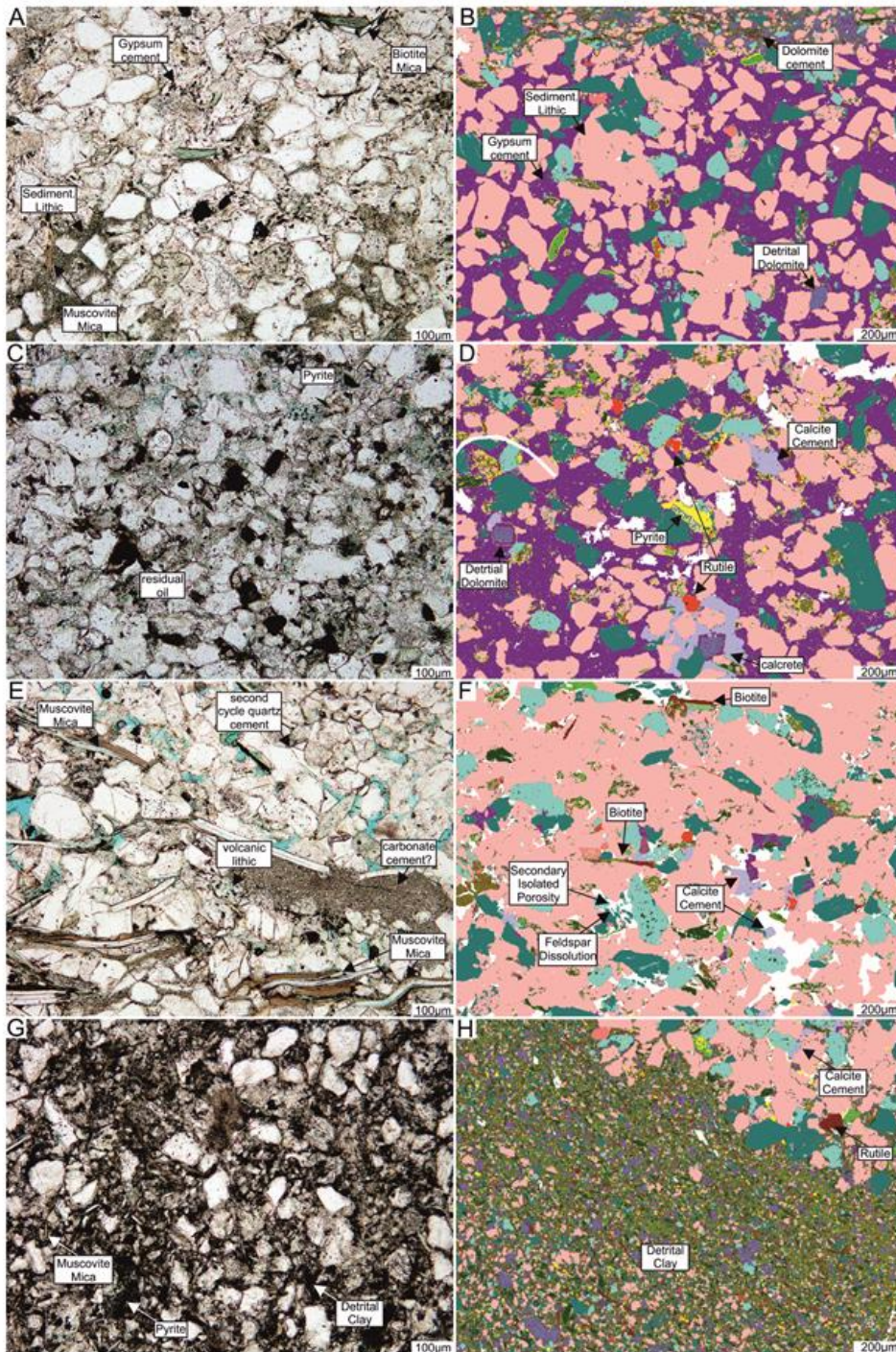


Figure 15.

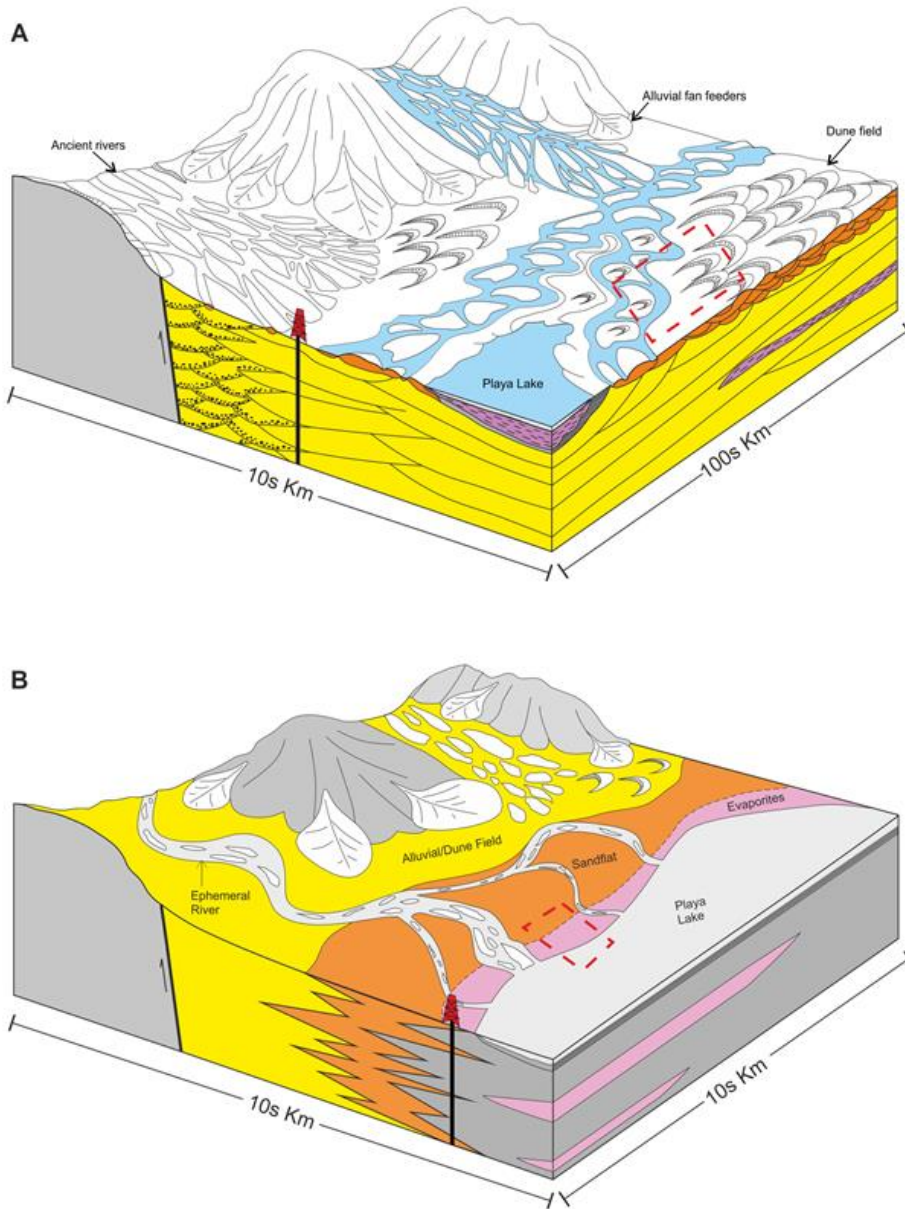


Figure 16.



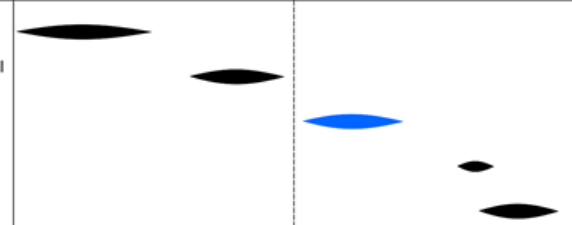

Ormskirk Sandstone Formation Diagenetic Phases	'EARLY'  Time  'LATER'
Carbonate cements Grain reorganisation and mechanical compaction Dissolution of unstable framework grains and pore-filling cement Pyrite Precipitation Residual oil	
Compaction (weak)	
Pore water chemistry	<p>Initial pore waters are likely to have been alkaline rich, leading to the precipitation of ferroan dolomite cements.</p> <p>Later pore waters are likely to have become increasingly acidic leading to dissolution of unstable framework grains. Pyrite locally precipitates during late diagenesis prior to oil emplacement.</p>
Porosity evolution and destruction	<p>Early ferroan dolomite cementation locally reduces porosity.</p> <p>Initial porosity loss occurs through grain reorganisation, (very weak to weak) compaction and infiltration of detrital clays.</p> <p>Porosity enhancement through the dissolution of unstable framework grains.</p>

Figure 17.

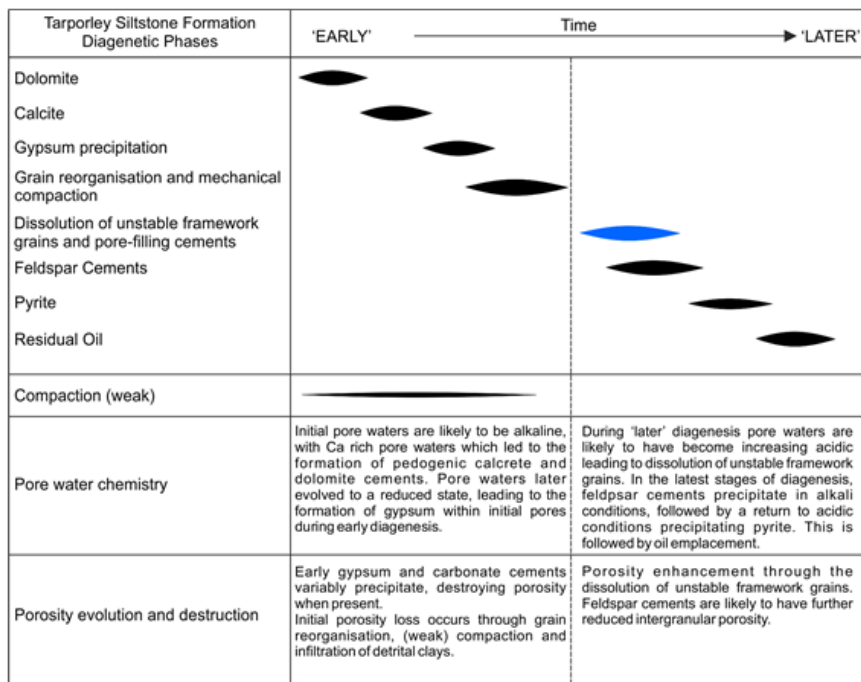


Figure 18

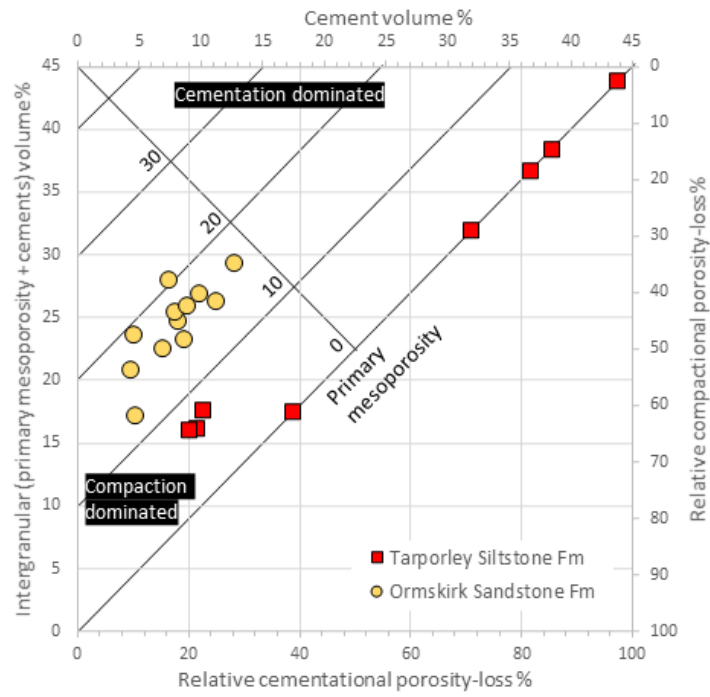




Figure 19

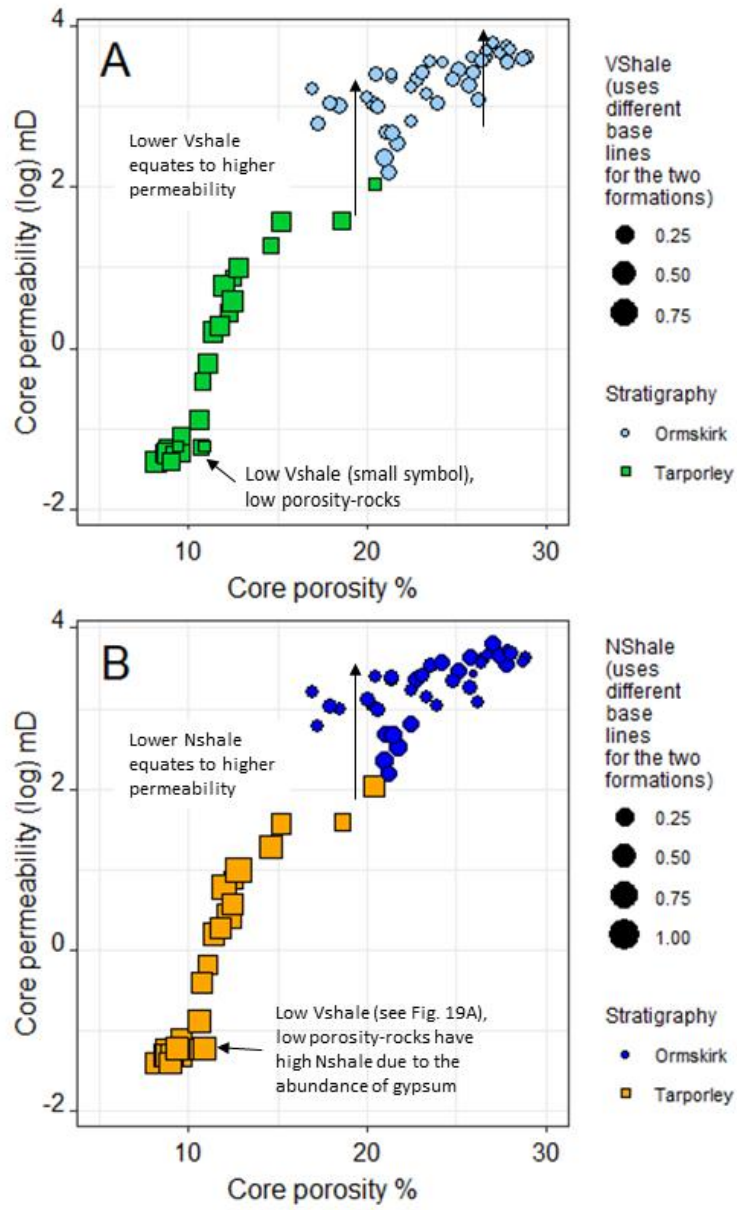


Figure 20

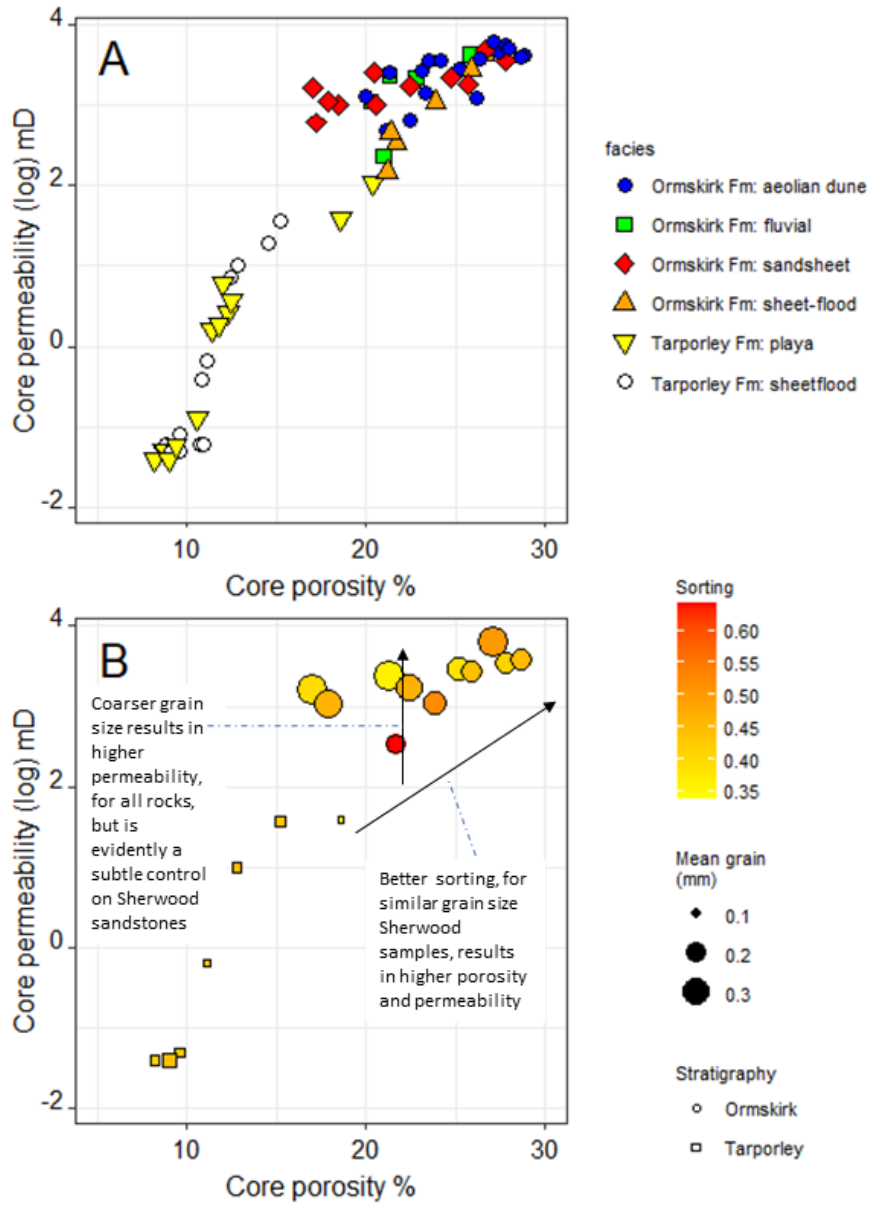


Figure 21

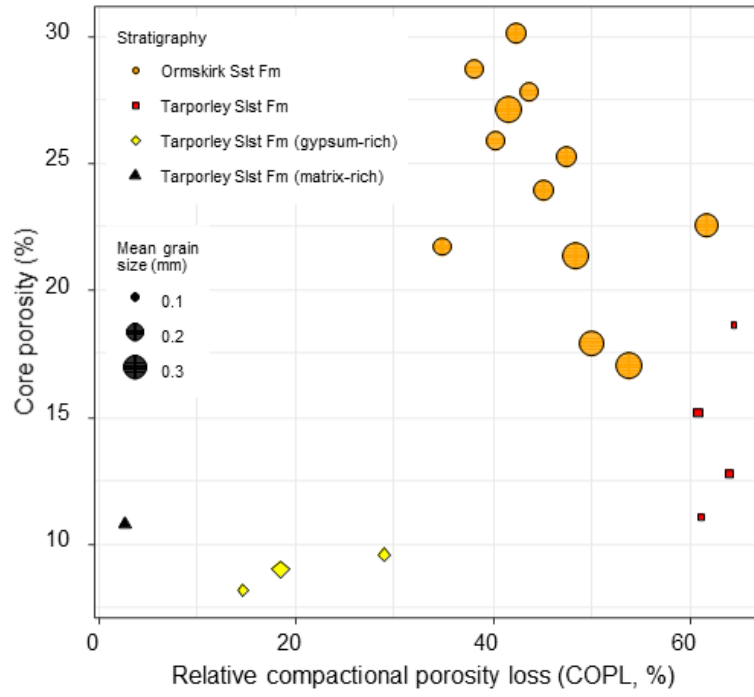


Figure 22

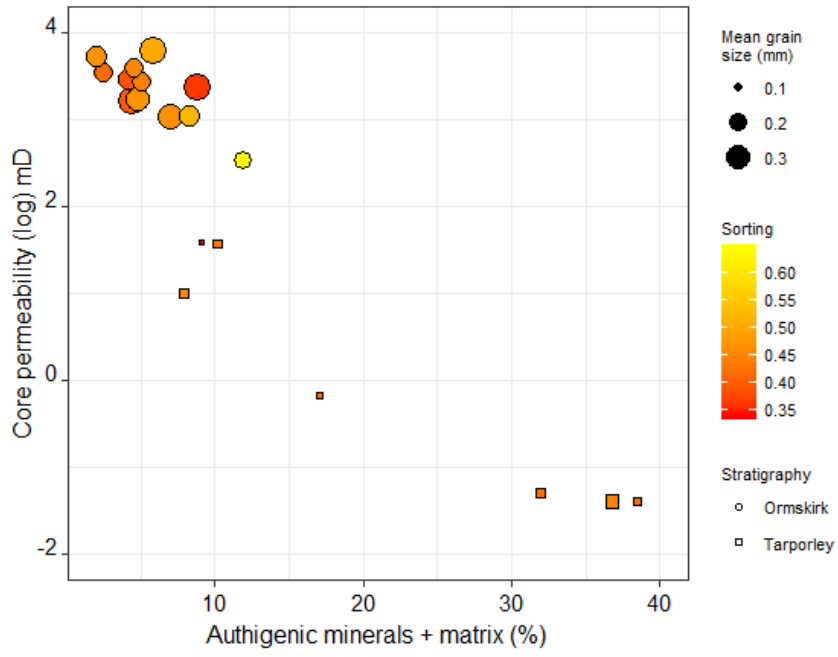


Table 1

Stratigraphy	Facies Code	Descriptions	Sedimentary structures	Bed type	Depositional environment
Ormskirk Sandstone Formation (Sherwood Sandstone Group)	AD	<b>Aeolian dune.</b> The facies is dark- to light brown (laminae alternating colours) and is characterised by grain size that ranges from fine- to medium grained. This facies contain high angle cross-stratification and local grain-fall laminae (Figure 11B). Bioturbation is absent. Bedding thickness is generally thin, but can range up to 2 m.	High angle cross-stratification and grain-fall laminae.	Homogenous Sandstone	Aeolian (minor fluvial reworking)
	FL	<b>Fluvial channel.</b> This facies is brown in colour and is characterised by grain size that ranges from medium- to coarse-grained. Planar cross-lamination and trough cross bedding is common throughout. Bioturbation is absent. Bedding thicknesses range from 10 cm to 40 cm.	Planar cross-lamination and trough cross bedding.	Homogenous Sandstone	Fluvial River
	SS	<b>Sand sheet.</b> This facies is mid- to dark brown in colour and is characterised by a grain size that ranges from fine- to medium grained. The facies are planar laminated, with some minor low angle cross-lamination and trough cross bedding observed. Bioturbation is absent. Bedding thicknesses generally range from 10 cm to 1m.	Laminated	Homogenous Sandstone	Aeolian - blown sand setting on a dry surface (minor fluvial reworking)
	SF	<b>Sand flat.</b> This facies is dark brown in colour and is characterised by a grain size that ranges from medium- to coarse grained. The facies are generally massive, with minor low-angle lamination and trough cross bedding observed. Bioturbation is absent. Bedding thicknesses generally range from 10- to 60 cm.	Massive, minor planar lamination and trough cross bedding.	Homogenous Sandstone	Aeolian - blown sand setting on a wet surface (minor fluvial reworking)
Tarporely Siltstone Formation (Mercia Mudstone Group)	SH	<b>Sheet flood.</b> This facies is dark brown in colour and is characterised by a grain size that ranges from fine silt- to fine sand grained. The facies generally have a mix of low-angle planar lamination and current ripples observed. Minor mudclasts and symmetrical ripples can also be seen. Bioturbation is absent. Bed thickness ranges up to 75 cm, and can combine to form stacked sequences up to 3 m in thickness.	Low-angle planar lamination and current ripples. Minor mudclasts and current ripples.	Heterogenous Sandstone / Siltstone	Lake-margin (lacustrine)
	PL	<b>Playa.</b> This facies is light- to mid grey coloured (alternating) and is characterised by grain size ranging from clay- to silt grained. Symmetrical (wave) ripples and planar lamination are common throughout. Desiccation cracks (Figure 11C) can be seen in some beds, which have been filled by later bed deposits. Bioturbation is absent. Individual laminations range up to 10 - 20 cm thickness, with multiple laminations combining to form stacked sequences up to 3- to 5 m in thickness.	Symmetrical wave ripples, desiccation cracks and planar laminations.	Heterogenous Claystone	Lacustrine

Table 2

<b>Control</b>	<b>Ormskirk Sandstone Formation</b>	<b>Tarporley Siltstone Formation</b>
<b>Grain size</b>	Medium grained sand (lower fine to coarse)	Silt (mud to very fine sand)
<b>Matrix content</b>	Negligible, low Vshale throughout, low Nshale throughout	Locally abundant, medium Vshale in sandy intervals, high Nshale in sandy intervals due to gypsum
<b>Early (eogenetic) cement type and content</b>	Minor dolomite	Locally abundant gypsum, where matrix is minimal, minor K-feldspar cement
<b>Compaction</b>	Dominant process controlling variable porosity	Matrix- and gypsum-rich beds have low compaction
<b>Dissolution of unstable detrital grains or earlier cement</b>	Minor, but possible dissolution of eogenetic gypsum	Minor
<b>Burial (mesogenetic) cement type and content</b>	None	None